



1 **A gridded dataset of consumptive water footprints, evaporation,** 2 **transpiration, and associated benchmarks related to crop production** 3 **in China during 2000-2018**

4 Wei Wang^{1,2}, La Zhuo^{1,2,3*}, Xiangxiang Ji⁴, Zhiwei Yue⁴, Zhibin Li^{1,2}, Meng Li⁴, Huimin Zhang⁴, Rong
5 Gao⁴, Chenjian Yan⁴, Ping Zhang⁴, Pute Wu^{1,2,3*}

6 ¹Institute of Soil and Water Conservation, Chinese Academy of Sciences and Ministry of Water Resources, Yangling 712100,
7 China

8 ²University of Chinese Academy of Sciences, Beijing 100049, China

9 ³Institute of Soil and Water Conservation, Northwest A&F University, Yangling 712100, China

10 ⁴College of Water Resources and Architectural Engineering, Northwest A&F University, Yangling 712100, China

11 *Correspondence to:* La Zhuo (zhuola@nwafu.edu.cn; lzhuo@ms.iswc.ac.cn), Pute Wu (gjzwpt@vip.sina.com).

12 **Abstract.** Evapotranspiration over crop growth period, also referred to as the consumptive water footprint of crop production
13 (WFCP), is an essential component of the hydrological cycle. However, the existing high-resolution consumptive WFCP
14 datasets do not distinguish between soil evaporation and crop transpiration and disregard the impacts of different irrigation
15 practices. This restricts the practical implementation of existing WFCP datasets for precise crop water productivity assessments,
16 agricultural water-saving evaluations, the development of sustainable irrigation techniques, cropping structure optimisation,
17 and crop-related interregional virtual water trade analysis. This study establishes a 5-arcmin gridded dataset of monthly green
18 and blue WFCP, evaporation, transpiration, and associated unit WFCP benchmarks for 21 crops grown in China during 2000-
19 2018. The data simulation was based on calibrated AquaCrop modelling under furrow-, sprinkler-, and micro-irrigated as well
20 as rainfed conditions. Data quality was validated by comparing the current results with multiple public datasets and remote-
21 sensing products. The improved gridded WFCP dataset effectively compensated for the gaps in the existing datasets through:
22 (i) revealing the intensity, structure, and spatiotemporal evolution of both productive and non-productive blue and green water
23 consumption on a monthly scale, and (ii) including crop-by-crop unit WFCP benchmarks according to climatic zones.

24 **1 Introduction**

25 The grain production potential of irrigated agriculture can effectively cope with the pressure that population growth places
26 on the food supply (Wada et al., 2013; Haddeland et al., 2014; Rosa et al., 2020; Puy et al., 2021; Wang et al., 2021) and
27 restrain the encroachment of cultivated land on natural regions (Tilman et al., 2011; Brown and Pervez, 2014; Jägermeyr et al.,
28 2017; Puy et al., 2020). Currently, irrigation accounts for more than 70% of worldwide blue water withdrawals (FAO, 2020)
29 and 90% of global water consumption (Döll, 2009). Irrigated cropland increases the soil water content and releases water



30 vapour into the atmosphere, leading to an alteration in the hydrological cycle (Rodell et al., 2009; Elliott et al., 2014; Leng et
31 al., 2014). Meanwhile, water scarcity is expected to increase in more than 80% of global farmlands, together with the
32 increasingly serious threats on sufficient agricultural water supply by the competition for water among sectors (Yin et al., 2017;
33 Pastor et al., 2019; Liu et al., 2022). Apparently, accurate assessment of water consumption on irrigated and rainfed farmlands
34 is crucial for identifying water-use hotspots and ensuring a stable food supply, particularly in the context of climate change.

35 The consumptive water footprint of crop production (WFCP) measures the consumption of blue water (i.e., irrigation
36 water extracted from surface and groundwater) and green water (i.e., soil water directly from rainfall) during the crop growth
37 period (Hoekstra and Chapagain, 2008; Hoekstra et al., 2011), permitting a unified evaluation of the water consumption of
38 irrigated and rainfed crops (Lovarelli et al., 2016). The most widely used WFCP database is the WaterStat (Hoekstra and
39 Mekonnen, 2012). It covers the WFCP of a wide variety of crops, crop derivatives, and biofuels, with data resolution at national,
40 watershed, and county spatial scales, but it only contains 10-year averages for 1996-2005 (WFN, 2022). The CWASI database
41 (Tamea et al., 2021) fills the resultant gap concerning the interannual evolution of WFCP data through a fast-track approach
42 (Tuninetti et al., 2017) at the national scale, suggesting that there is significant interannual variation in the water footprint per
43 unit mass of crop production (uWFCP), which should be taken into account in analyses and applications. However, none of
44 the aforementioned studies have considered intra-annual variations or intra-national differences in agricultural water
45 consumption. Considering that disparities in space and time in the WFCP and uWFCP may have various effects on the
46 formulation of water management measures. Such changes must be evaluated to provide a reference for seasonal water
47 shortages (Hoekstra, 2013; Zhuo et al., 2016c).

48 Numerous studies have assessed the blue and green WFCP of specific crops at finer spatial and temporal resolutions using
49 the agro-hydrological models including CROPWAT (Mekonnen and Hoekstra, 2011; Tuninetti et al., 2015), GEPIC (Liu et al.,
50 2007), GCWM (Siebert and Döll, 2010), LPJmL (Fader et al., 2011), and AquaCrop (Zhuo et al., 2016b; Wang et al., 2019).
51 Utilising the WATNEEDs model, Chiarelli et al. (2020) produced the first dataset to record global monthly blue and green
52 water requirements of producing 23 crops at a 5 arcmin scale. They found that green water accounts for 84% of the considered
53 global crop water requirements. However, the actual water consumption during crop production is frequently less than the
54 predicted water requirement owing to soil water deficit, insufficient precipitation, and differences in field management (Long
55 and Singh, 2013; Fisher et al., 2017). Furthermore, the aforementioned datasets ignore the non-negligible differences between
56 the WFCP when using different water supply modes or irrigation practices and do not distinguish between the blue and green
57 water consumption of two independent processes, namely soil evaporation (that is extravagant water consumption) and crop
58 transpiration. In summary, the limitations of existing WFCP databases mean that they cannot be used to evaluate the effect of
59 implementing water-saving irrigation practices on the spatiotemporal distribution of agricultural water consumption at a large



60 regional scale (Wang et al., 2019). Moreover, the lack of information on extravagant water consumption of crops in terms of
61 the water sources and the spatiotemporal distribution hinders the precise implementation of water-saving agricultural policies
62 and technologies (Jung et al., 2010; Lian et al., 2018).

63 To fill the abovementioned gaps in existing WFCP datasets, we developed a gridded dataset comprising monthly green
64 and blue WFCP, evaporation and transpiration, and associated uWFCP benchmarks for 21 crops grown in China during 2000-
65 2018. A self-sufficiency-oriented food policy has fuelled the explosive growth of water-saving irrigated farmlands in China in
66 recent decades (SCIO, 1996; Ghose, 2014), with water-saving irrigated areas increasing by 5,698 kha from 2000 to 2018
67 (representing 12% of the total irrigated area in 2018) (NBSC, 2022). The current study followed the WFN accounting
68 framework (Hoekstra et al., 2011) and used the calibrated AquaCrop model to simulate the monthly WFCP at a resolution of
69 5 arcmin. The considered 21 crops account for 83% of national sown areas and 75% of national crop production in China
70 (NBSC, 2022). The dataset differs from the others in four aspects: (i) It evaluated the effects of different water supply modes
71 (irrigated or rain-fed) and irrigation practices (furrow, sprinkler, and micro-irrigation) on water consumption throughout the
72 crop growth period. (ii) It distinguished between monthly blue and green water consumption via soil evaporation and crop
73 transpiration. (iii) The dataset encompassed both the WFCP in $\text{m}^3 \text{yr}^{-1}$ and the uWFCP in $\text{m}^3 \text{ton}^{-1}$. (iv) It identified uWFCP
74 benchmarks that differentiated between various climatic zones and irrigation practices. The data quality was verified through
75 its comparison with available public databases and remote sensing products.

76 2 Data and methods

77 Three main steps were followed to create and validate the WFCP dataset under various water supply modes and irrigation
78 practices during 2000-2018 (Fig. 1).

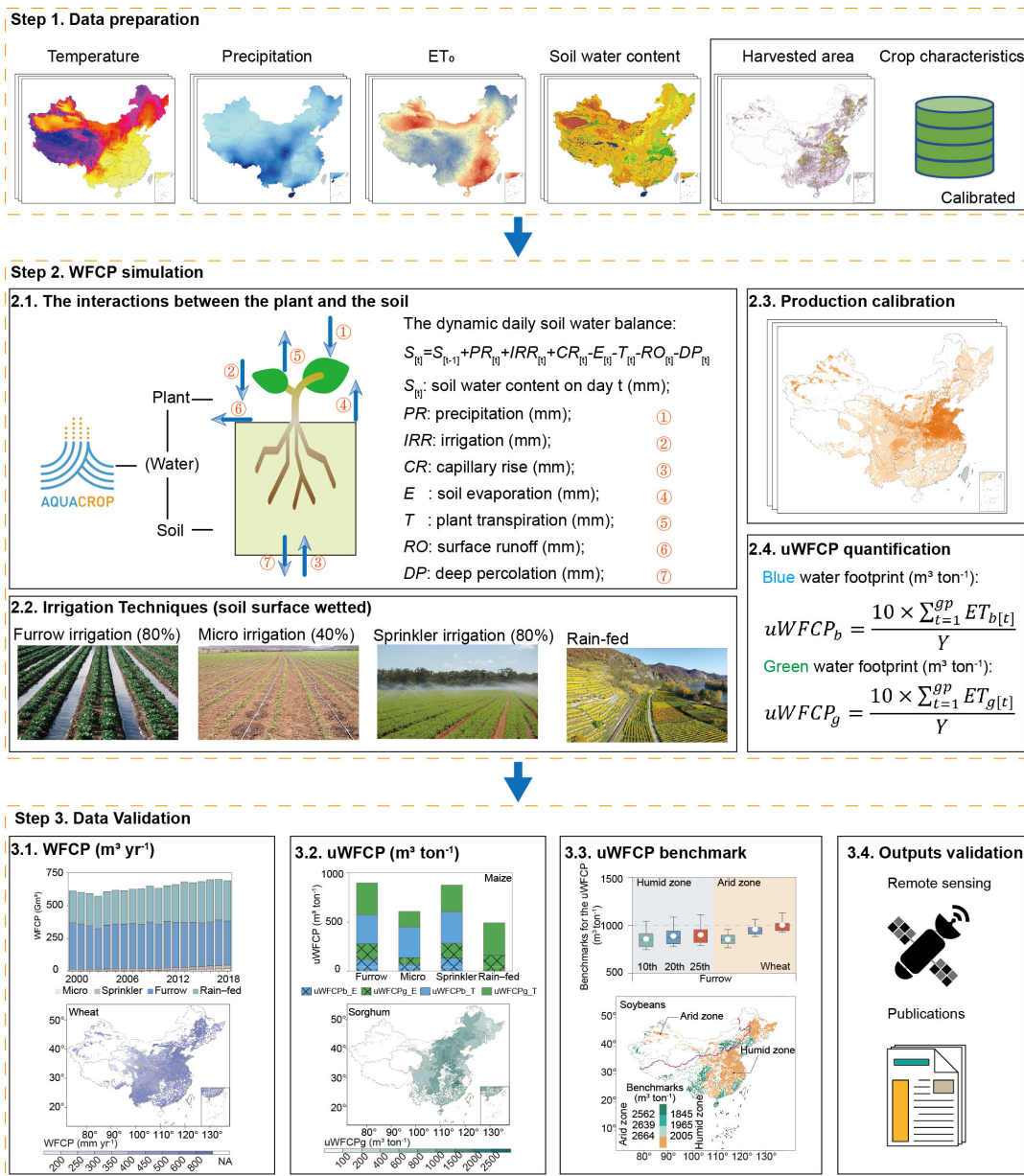
79 **Step 1: Data preparation.** We collected, verified, and inverted data on the yearly planting area of each crop under various
80 water supply modes and irrigation practices at a resolution of 5 arcmin. The AquaCrop simulation required monthly
81 precipitation, temperature, reference evapotranspiration (ET_0), and CO_2 datasets. The calibrated crop parameters were obtained
82 from the published literature.

83 **Step 2: Water footprint simulation.** The AquaCrop model was run with daily steps to simulate soil evaporation, crop
84 transpiration, and crop yield during the growth period of crops. The WFCP and uWFCP were calculated for different water
85 supply modes and irrigation practices using a spatial resolution of 5 arcmin and a temporal resolution of months (Zhuo et al.,
86 2016c; Wang et al., 2019).

87 **Step 3: Data validation.** The simulation results were verified by comparing them with remote sensing products of actual



88 evapotranspiration (Cheng et al., 2021) and publicly accessible WFCP datasets (Mekonnen and Hoekstra, 2011; Zhuo et al.,
 89 2016a; Chiarelli et al., 2020).
 90



91
 92

Figure 1. Three main steps for quantifying the water footprint of crop production.



93 **2.1 Data sources**

94 **2.1.1 Crop planting area and production**

95 The irrigated and rain-fed areas of each crop from 2001 to 2018 were assigned at a resolution of 5 arcmin according to
96 the base map for the year 2000 obtained from the MIRCA2000 dataset (Portmann et al., 2010) and interannual changes per
97 province extracted from the China Statistical Yearbook (NBSC, 2022). At the provincial scale, irrigation data from 2000-2018
98 were spatially divided into the proportional areas in which furrow, sprinkler, and micro-irrigation was used for each crop,
99 retrieving data from the statistical yearbook (CAMIYC, 2022). Due to the lack of data in this regard, all vegetables were
100 assumed to be grown under irrigation as based on agricultural practice. The national production data for tomatoes and cabbage
101 were derived from the Food and Agriculture Organization dataset (FAO, 2022) and was proportionally allocated to vegetable
102 production by provinces. Production data for the remaining crops were obtained from the NBSC (2022).

103 **2.1.2 Meteorological and soil data**

104 The monthly data for precipitation, minimum and maximum temperature, and reference evapotranspiration were obtained
105 from the Climatic Research Unit Time-Series 4.06 dataset (Harris et al., 2020). All meteorological data were resampled to a 5
106 arcmin spatial resolution using the ArcGIS mapping platform. Atmospheric CO₂ concentration data were acquired from the
107 Mauna Loa Observatory in Hawaii (Tans and Keeling, 2020). Soil texture data were obtained from the International Soil
108 Reference and Information Centre (ISRIC) soil profile database (Dijkshoorn et al., 2008). Soil water content data were obtained
109 from the ISRIC World Inventory of Soil Emission Potentials database (Batjes, 2012). Table 1 summarizes the data sources.

110

111 **Table 1. Inventory of data sources.**

Variables	Data source	Spatial resolution	Period	Data link
Irrigated and rainfed crop areas	MIRCA 2000	5 arcmin	2000-2018	https://www.uni-frankfurt.de/45218031/Data_download_center_for_MIRCA2000
Crop production, yield and harvested areas	NBSC	Provincial	2000-2018	https://data.stats.gov.cn/adv.htm?m=advquery&cn=E0103
Production of vegetables	FAOSTAT	National	2000-2018	https://www.fao.org/faostat/en/#data/QV
Area of different irrigation techniques	CAMIY	Provincial	2000-2018	https://data.cnki.net/Trade/yearbook/single/N2021040192?zcode=Z032
Meteorological data	CRU TS v. 4.03	30 arcmin	2000-2018	https://crudata.uea.ac.uk/cru/data/hrg/
CO ₂ concentration	NOAA	Average	2000-2018	https://gml.noaa.gov/ccgg/trends/data.html



Soil texture	ISRIC	1 arcmin	-	https://data.isric.org/geonetwork/srv/eng/catalog.search#/met adata/2919b1e3-6a79-4162-9d3a-e640a1dc5aef
Initial soil moisture content	ISRIC	5 arcmin	-	https://data.isric.org/geonetwork/srv/eng/catalog.search#/met adata/82f3d6b0-a045-4fe2-b960-6d05bc1f37c0

112 Note: “-” means constant values.

113

114 2.1.3 Crop characteristics

115 The characteristics of crops selected for this study are listed in Table 2. Due to differences in their phenology, wheat,
 116 maize, barley, and rapeseed had two sowing periods, whereas rice had three sowing periods across the study’s time frame. The
 117 growth period of all crops was divided into four stages based on their growth characteristics (Allen et al., 1998; Vanuytrecht
 118 et al., 2014): the initial (L1), crop development (L2), mid-season (L3), and late-season (L4) growth stages. Crop planting dates
 119 were retrieved from Chen et al. (1995), the reference harvest index from Xie et al. (2011) and Zhang and Zhu (1990), and crop
 120 growth stages and maximum root depth from Allen et al. (1998) and Hoekstra and Chapagain (2006).

121

122 **Table 2. Crop characteristics for the 21 crops in China.**

Crop class	Crop code	Planting date	Length of crop development stage (day)				Root deeps (m)		WP*	HI ₀
			L1	L2	L3	L4	Irrigated	Rainfed		
Wheat	1									
Spring wheat		15th Mar	20	25	60	30	1	1.5	15	39
Winter wheat		15th Oct	30	140	40	30	1.5	1.8	15	40
Maize	2									
Spring maize		15th Apr	30	40	50	30	1	1.7	33.7	44
Summer maize		1st Jun	20	35	40	30	1	1.7	33.7	43
Rice	3									
Early rice		15th Mar	30	30	30	30	0.5		19	44
Mid rice		15th Apr	30	30	60	30	0.5		19	44
Late rice		15th Jul	30	30	70	40	0.5		19	44
Sorghum	4	1st May	20	35	45	30	1	2	33.7	39
Millet	5	15th Apr	15	55	40	20	1	1.5	32	47
Barley	6									
Spring barley		15th Apr	15	35	50	30	1	1.5	15	39
Winter barley		25th Oct	20	110	40	35	1	1.5	15	39
Soybeans	7	1st Jun	20	40	60	30	0.6	1.3	15	44
Potatoes	8	1st May	25	30	45	30	0.4	0.6	18	69
Sweet potatoes	9	1st May	20	30	60	40	1	1.5	18	59
Cotton	10	1st Apr	30	50	55	45	1	1.7	15	38



Sugar cane	11	1st Feb	30	50	180	60	1.2	2	30	60
Sugar beets	12	15th Apr	50	40	50	40	0.7	1	17	71
Groundnuts	13	15th Apr	10	80	35	25	0.5	1	17	43
Rapeseed	14									
Spring rapeseed		15th Apr	6	69	20	36	0.8	1.5	17	32
Winter rapeseed		30th Sep	6	148	20	36	0.8	1.5	17	32
Sunflower	15	15th Apr	25	35	45	25	0.8	1.5	18	31
Tomatoes	16	15th Jan	30	40	40	25	0.7	1.5	18	40
Apple	17	1st Mar	30	50	130	30	1	2	20	20
Tea	18	15th Feb	120	60	180	5	0.9	0.9	17	5
Tobacco	19	15th May	20	30	30	30	0.8	0.8	17	61
Cabbage	20	5th Jul	40	60	50	15	0.5	0.8	15	67
Grapes	21	1st Apr	30	60	40	80	1		17	2

123

124 2.2 Methods

125 2.2.1 Calculation of uWFCP

126 The blue and green uWFCP were obtained from the blue and green components of the WFCP (evapotranspiration during
 127 the crop growth period) in relation to the crop yield (Hoekstra et al., 2011).

$$128 \quad uWFCP_b = \frac{10 \times \sum_{t=1}^{gp} ET_{b[t]}}{Y} \quad (1)$$

$$129 \quad uWFCP_g = \frac{10 \times \sum_{t=1}^{gp} ET_{g[t]}}{Y} \quad (2)$$

130 where $uWFCP_b$ and $uWFCP_g$ are the blue and green uWFCP, respectively ($m^3 \text{ ton}^{-1}$); ET_b and ET_g are the blue and green
 131 WFCP (that is, $WFCP_b$ and $WFCP_g$), respectively (mm) (see equations 8 and 9); gp represents the days in the growing period;
 132 10 is the unit conversion factor; Y (see equation 4 below) is the crop yield (ton ha^{-1}); and t indicates a given day.

133 The daily aboveground biomass production (B) was obtained as follows:

$$134 \quad B = WP^* \times \sum \frac{Tr_{[t]}}{ET_{0[t]}} \quad (3)$$

135 where WP^* ($\text{ton ha}^{-1} \text{ mm}^{-1}$) expresses the aboveground dry matter produced per unit land area per unit of transpired water,
 136 which is governed by a combination of atmospheric CO_2 concentration, crop type (C3 and C4 crops), and soil fertility. The
 137 WP^* is multiplied with the ratio of crop transpiration (Tr) to the reference evapotranspiration (ET_0) for that day. The goal of
 138 normalisation is to make WP^* applicable to diverse locations and seasons, including future climate scenarios.

139 The crop yield (Y) (ton ha^{-1}) was obtained by multiplying the aboveground biomass (B) with an adjusted reference harvest
 140 index:

$$141 \quad Y = f_{HI} HI_0 B \quad (4)$$



142 where f_{HI} is the calibration coefficient of the standardised harvest index HI_0 , which is influenced by water stress and
 143 temperature stress.

144 2.2.2 Dynamic daily soil water balance

145 By tracking the daily incoming and outgoing water fluxes at the root zone boundary, the dynamic daily soil water balance
 146 was calculated as follows (Mekonnen and Hoekstra, 2010):

$$147 \quad S_{[t]} = S_{[t-1]} + PR_{[t]} + IRR_{[t]} + CR_{[t]} - ET_{[t]} - RO_{[t]} - DP_{[t]} \quad (5)$$

148 where S is the soil water content (mm); PR is the precipitation (mm); IRR is the irrigation water volume (mm); CR is the
 149 capillary rise from groundwater, assumed to be zero (mm); RO is the surface runoff (mm); DP is the deep soil percolation
 150 (mm); and ET is the actual evapotranspiration (mm), consisting of soil evaporation (E) and crop transpiration (Tr), which were
 151 calculated as follows:

$$152 \quad E = (K_r K_e) ET_0 \quad (6)$$

$$153 \quad Tr = (K_s K_{S_{Tr}} K_{C_{Tr}}) ET_0 \quad (7)$$

154 where K_r is the evaporation reduction coefficient, which is less than 1 (dimensionless); K_e is the soil evaporation
 155 coefficient, which is proportional to the fraction of the soil surface not covered by the canopy (dimensionless); K_s is the soil
 156 water stress coefficient, which is smaller than 1 when there is insufficient soil water to meet the evaporative demand of the
 157 atmosphere (dimensionless); $K_{S_{Tr}}$ is the cold stress coefficient, which drops below 1 when the temperature is insufficient for
 158 growth (dimensionless); and $K_{C_{Tr}}$ is the crop transpiration coefficient, which is proportional to the green canopy cover
 159 (dimensionless).

160 By tracking the proportional contribution of daily rainfall and irrigation water to each element of the soil water balance,
 161 $ET_{b[t]}$ and $ET_{g[t]}$ were extracted (Zhuo et al., 2016c; Chukalla et al., 2015):

$$162 \quad ET_{b[t]} = IRR_{[t]} + S_{b[t-1]} - S_{b[t]} - RO_{[t]} \left(\frac{IRR_{[t]}}{PR_{[t]} + IRR_{[t]}} \right) - DP_{[t]} \left(\frac{S_{b[t-1]}}{S_{[t-1]}} \right) \quad (8)$$

$$163 \quad ET_{g[t]} = PR_{[t]} + S_{g[t-1]} - S_{g[t]} - RO_{[t]} \left(\frac{PR_{[t]}}{PR_{[t]} + IRR_{[t]}} \right) - DP_{[t]} \left(\frac{S_{g[t-1]}}{S_{[t-1]}} \right) \quad (9)$$

164 where $S_{b[t]}$ and $S_{g[t]}$ are the blue and green soil water content (mm) for a crop, respectively, at the end of day t . Following
 165 Zhuo et al. (2016c), the green water value was used as the initial soil water content in each calculation cell.

166 2.2.3 Irrigation practices module

167 Different irrigation practices indirectly affect water consumption during the growth period due to differences in the
 168 fraction of the surface wetted (f_w) by each method (Raes et al., 2018). The soil evaporation coefficient (K_e) was multiplied by



169 the f_w -value to account for partial wetness when only a portion of any soil surface was irrigated. Owing to special environmental
170 restrictions, furrow irrigation was used for rice planting in this study. Specific irrigation conditions were divided into either
171 sufficient or water-demanding subtypes (irrigation to field capacity when the soil water content reached the wilting point).

$$172 \quad K_e = f_w(1 - CC^*)K_{e_x} \quad (10)$$

$$173 \quad (1 - CC^*) = 1 - 1.72CC + CC^2 - 0.3CC^3 \quad \geq 0 \quad (11)$$

174 where the f_w -values used for furrow, sprinkler, and micro-irrigation were 80%, 100%, and 40%, respectively; $(1 - CC^*)$
175 is the dimensionless adjusted fraction of the non-covered soil surface (dimensionless); and K_{e_x} is the maximum soil
176 evaporation coefficient (dimensionless) for fully wet and non-shaded soil surfaces.

177 2.2.4 Benchmarks for uWFCP

178 The uWFCP of each grid in the same climate zone was ranked from lowest to highest, and the uWFCP corresponding to
179 a cumulative crop production of 10%, 20% and 25% of the total production were recorded as the regional uWFCP benchmarks
180 (Mekonnen and Hoekstra, 2014; Zhuo et al., 2016b; Wang et al., 2019; Yue et al., 2022). Climate zone is a key factor
181 influencing regional uWFCP benchmarks (Zhuo et al., 2016b). Therefore, we classified China's climatic regions based on the
182 aridity index (Middleton and Thomas, 1997) (AI; defined as the ratio of rainfall to reference evapotranspiration) and set up
183 regional uWFCP benchmarks for humid (AI > 0.5) and arid (AI < 0.5) zones.

184 2.3 Calibration and validation

185 2.3.1 Production calibration

186 The statistical yearbook only has crop production statistics on the provincial level. Therefore, we calibrated crop
187 production at the provincial scale, using a grid scale depicting different water supply modes and irrigation practices based on
188 the proportional relationship (R) between yield simulation results and the NBSC data (Mialyk et al., 2022).

$$189 \quad R = \frac{P_{P_{sta}}}{\sum_{i=1}^4 P_{G_{i,sim}}} \quad (12)$$

$$190 \quad P_{G_{i,act}} = P_{G_{i,sim}} \cdot R \quad (13)$$

191 where $P_{P_{NBSC}}$ is the statistical (sta) provincial crop production (ton yr⁻¹); i represents the water supply modes and
192 irrigation practices; $P_{G_{i,sim}}$ is the simulated (sim) grid crop production value (ton yr⁻¹) according to i ; and $P_{G_{i,act}}$ is the actual
193 (act) grid crop production value (ton yr⁻¹) according to i .



194 2.3.2 Remote sensing validation

195 Because of the spatially fragmented nature of crop cultivation, we conducted remote sensing validation according to the
196 Chinese Agricultural Cropping System to reduce the interference of non-agricultural land with the validation results (IGSNRR,
197 2022). We selected grids in which the sum of planted areas was greater than 5 kha (> 50% of a single grid) and greater than 10
198 kha (>100% of a single grid) for single- and multi-crop regions, respectively. In terms of the time span, 19 of the 21 crops
199 studied experienced growth periods from April to August; therefore, these five months were set as the validation interval in
200 terms of total evapotranspiration.

201 2.3.3 Publications comparison

202 The present dataset was compared with published studies that included temporal and spatial data overlaps. The
203 comparison included the crop planting area at the grid scale (Cheng et al., 2021; Grogan et al., 2022), and the WFCP and
204 uWFCP values at the grid and national scale (Mekonnen and Hoekstra, 2011; Zhuo et al., 2016a; Chiarelli et al., 2020).

205 2.3.4 Accuracy assessment

206 The linear regression coefficient (R^2) was used to measure the consistency between the statistical data, remote sensing
207 data, and simulated results. A greater R^2 value indicates a better match.

$$208 \quad R^2 = \frac{(\sum_{i=1}^n (x_i - \bar{x}_i) \times (\text{ref}_i - \overline{\text{ref}}_i))^2}{\sum_{i=1}^n (x_i - \bar{x}_i)^2 \times \sum_{i=1}^n (\text{ref}_i - \overline{\text{ref}}_i)^2} \quad (13)$$

209 where n indicate the number of samples; x_i and ref_i represent the simulated and statistical values (remote sensing data),
210 respectively; \bar{x}_i and $\overline{\text{ref}}_i$ are the mean values of the simulated and statistical values (remote sensing data), respectively.

211 3 Results

212 3.1 Water footprint of crop production

213 During the study period, the WFCP of 21 crops in China increased by 13% to 690 Gm³ yr⁻¹ in 2018, with WFCP_b and
214 WFCP_g accounting for 29% and 71% of this increase, respectively. The WFCP_b and WFCP_g varied greatly across crops, time,
215 and space. Table 3 presents the WFCP of the 21 crops under different water supply modes and irrigation practices. Maize (165
216 Gm³ yr⁻¹), rice (143 Gm³ yr⁻¹), and wheat (125 Gm³ yr⁻¹) had the highest WFCP, accounting for 67% of the total WFCP. The
217 WFCP of grapes (177%) and maize (94 Gm³ yr⁻¹) showed the greatest growth rate, with their planting areas expanding by 156%
218 and 82%, respectively (NBSC, 2022).



219 **Table 3. WFCP and planting area under different water supply modes and irrigation practices for 21 crops.**

Crop	Furrow irrigation			Micro irrigation			Sprinkler irrigation			Rain-fed	
	WFCP _b	WFCP _g	Area	WFCP _b	WFCP _g	Area	WFCP _b	WFCP _g	Area	WFCP _g	Area
	M m ³	M m ³	k ha	M m ³	M m ³	k ha	M m ³	M m ³	k ha	M m ³	k ha
	(△)	(△)	(△)	(△)	(△)	(△)	(△)	(△)	(△)	(△)	(△)
Wheat	40,595	35,702	13,157	4,384	2,369	1,357	2,170	1,583	625	41,046	9,127
	(-22%)	(-9%)	(-18%)	(1936%)	(1650%)	(1964%)	(-26%)	(-10%)	(-20%)	(5%)	(-6%)
Maize	31,023	40,092	13,122	5,581	3,604	1,611	4,351	4,413	1,538	120,279	25,859
	(3%)	(18%)	(12%)	(4577%)	(2950%)	(3413%)	(67%)	(107%)	(95%)	(162%)	(147%)
Rice	81,847	58,979	28,306	-	-	-	4,629	5,540	1,883	-	-
	(4%)	(1%)	(-4%)	-	-	-	(329%)	(404%)	(366%)	-	-
Sorghum	346	457	157	57	46	21	53	53	20	1,757	424
	(-36%)	(-20%)	(-27%)	(3124%)	(2259%)	(2583%)	(34%)	(85%)	(66%)	(-35%)	(-36%)
Millet	346	388	137	43	32	16	46	42	16	2,652	609
	(-27%)	(-10%)	(-20%)	(2176%)	(1786%)	(2032%)	(10%)	(41%)	(28%)	(-38%)	(-43%)
Barley	91	133	67	14	12	7	6	7	3	768	235
	(-48%)	(-48%)	(-52%)	(4024%)	(3355%)	(2902%)	(-3%)	(3%)	(-13%)	(-67%)	(-65%)
Soybeans	3,936	6,751	1,963	413	375	144	389	609	193	27,319	6,113
	(-22%)	(-16%)	(-19%)	(2315%)	(1871%)	(2031%)	(35%)	(102%)	(88%)	(-7%)	(-10%)
Potatoes	721	966	377	140	78	39	91	88	34	16,171	4,440
	(-20%)	(11%)	(14%)	(3694%)	(2962%)	(3256%)	(50%)	(121%)	(106%)	(8%)	(1%)
Sweet potatoes	873	1,653	427	37	57	16	37	59	16	10,276	1,921
	(-64%)	(-55%)	(-57%)	(429%)	(561%)	(513%)	(-67%)	(-44%)	(-51%)	(-60%)	(-60%)
Cotton	2,195	2,268	625	788	217	134	85	82	23	9,824	2,573
	(-54%)	(-45%)	(-52%)	(4353%)	(1770%)	(3006%)	(-59%)	(-37%)	(-49%)	(-27%)	(-5%)
Sugar cane	258	589	98	9	20	3	8	17	3	10,924	1,302
	(-36%)	(-37%)	(-40%)	(1309%)	(1196%)	(1145%)	(163%)	(170%)	(150%)	(32%)	(28%)
Sugar beets	0.096	0.029	0.021	0.145	0.043	0.056	0.003	0.001	0.002	812	216
	(-78%)	(-78%)	(-72%)	(5530%)	(5859%)	(12331%)	(-85%)	(-85%)	(-61%)	(-34%)	(-34%)
Groundnuts	3,500	4,842	1,435	209	178	66	210	223	72	14,441	3,046
	(-6%)	(4%)	(-3%)	(1776%)	(1596%)	(1587%)	(11%)	(62%)	(42%)	(-6%)	(-8%)
Rapeseed	0.0159	0.0539	0.0147	0.0001	0.0002	0.0001	0.0001	0.0005	0.0001	19,053	6,551
	(256%)	(37%)	(67%)	(3336%)	(1653%)	(1800%)	(2660%)	(965%)	(1194%)	(3%)	(-13%)
Sunflower	262	202	87	137	49	33	34	21	10	2,913	792
	(-35%)	(-16%)	(-26%)	(8591%)	(5601%)	(6626%)	(-1%)	(22%)	(10%)	(-25%)	(-28%)
Tomatoes	1,365	1,581	949	74	57	44	74	69	47	-	-
	(48%)	(60%)	(45%)	(2379%)	(2463%)	(2270%)	(109%)	(198%)	(144%)	-	-
Apple	2,366	2,223	568	352	226	85	166	134	36	7,551	1,250
	(-47%)	(-32%)	(-41%)	(1638%)	(1236%)	(1452%)	(-53%)	(-37%)	(-44%)	(11%)	(2%)
Tea	2,218	3,200	550	51	86	15	68	92	16	13,803	1,730
	(65%)	(46%)	(43%)	(1690%)	(1622%)	(1464%)	(427%)	(453%)	(404%)	(242%)	(252%)
Tobacco	308	673	201	13	39	12	14	26	8	3,819	836
	(-30%)	(-12%)	(-18%)	(1181%)	(1800%)	(1848%)	(-34%)	(21%)	(4%)	(-28%)	(-29%)
Cabbage	1,523	2,642	897	72	96	42	76	124	45	-	-
	(-18%)	(-19%)	(-24%)	(1183%)	(1033%)	(1136%)	(15%)	(47%)	(28%)	-	-
Grapes	0.013	0.006	0.003	0.033	0.015	0.008	0.0004	0.0002	0.0001	3,869	725
	(-58%)	(-59%)	(-58%)	(17901%)	(17826%)	(18248%)	(-71%)	(-71%)	(-71%)	(177%)	(156%)

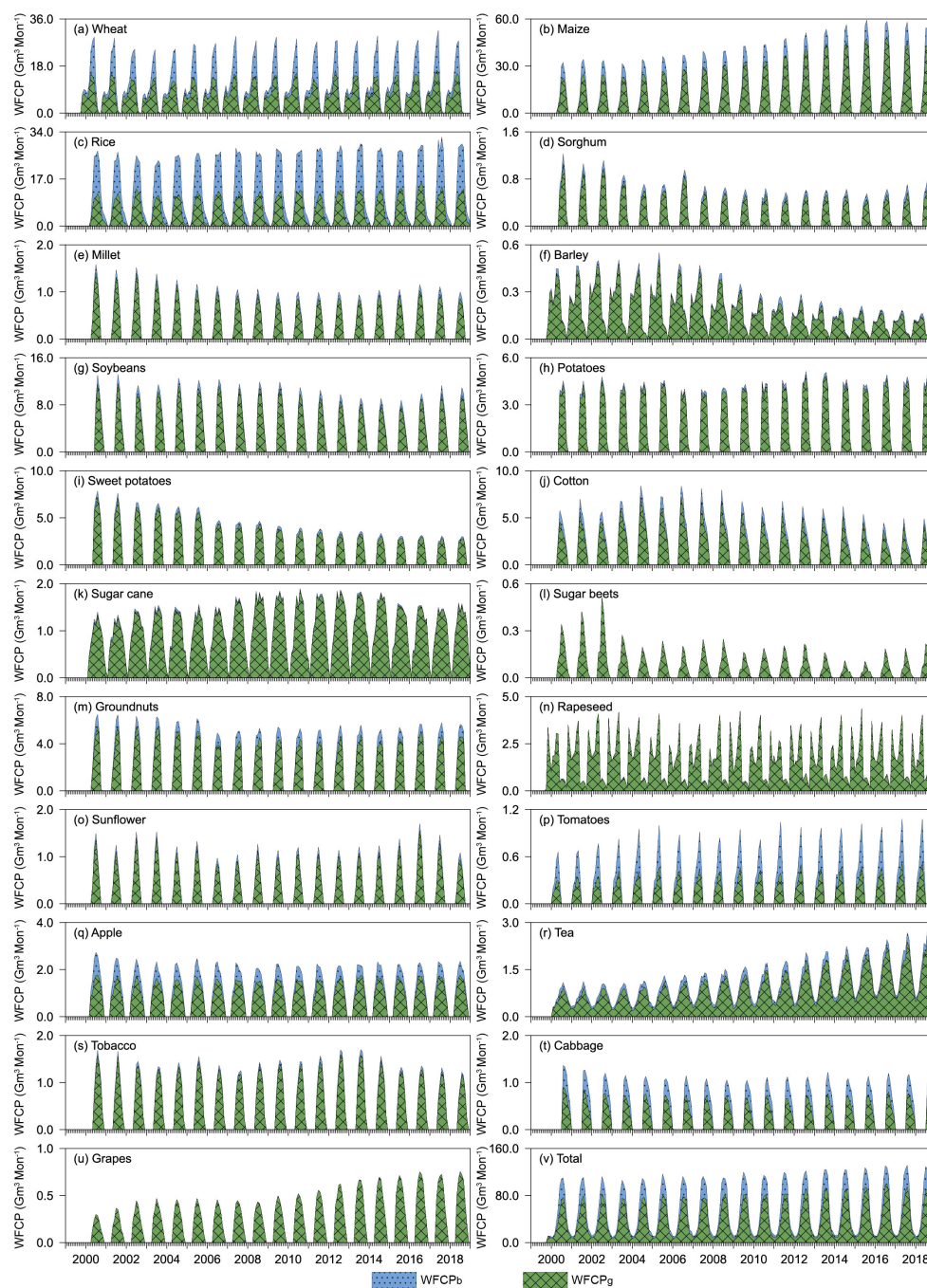
220 Note: “△” refers to the rate of change from 2000 to 2018. “-” indicates that no crops are grown.

221

222 In addition, the annual average proportions of WFCP attributable to furrow irrigation and rain-fed conditions reached 53%
 223 and 44%, respectively (Fig. S1). Nevertheless, the WFCP of sprinkler and micro-irrigation expanded by 11 and 19 Gm³ yr⁻¹,
 224 respectively, increasing their proportional contribution to the total WFCP by respective factors of 1.6 and 23. Over the same
 225 period, WFCP under furrow irrigation decreased by 5%. Therefore, sprinklers and micro-irrigation planting modes are being



226 deployed more often on existing and freshly reclaimed farmland in China (NBSC, 2022). In conclusion, when quantifying and
 227 evaluating the WFCP, it is vital to consider the influence of various water supply modes and irrigation practices (Wang et al.,
 228 2019).



229

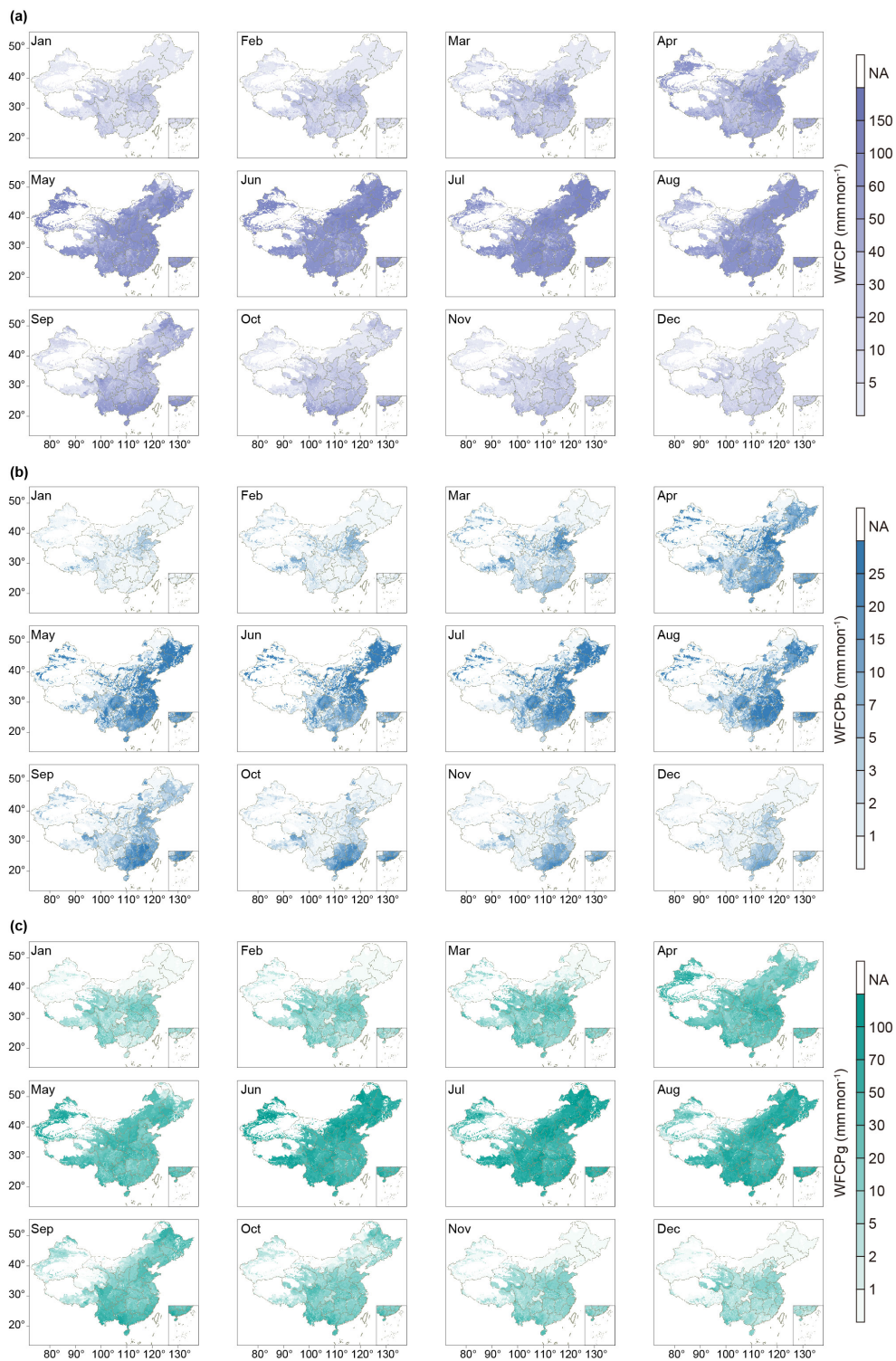
230 **Figure 2. Total national monthly WFCP_g and WFCP_b of 21 crops in China over 2000-2018.**



231 The water source accessed for crop production varied cyclically across years (Fig. 2). The $WFCP_b$ peaked annually in
232 May, with an average annual value of $16 \text{ Gm}^3 \text{ mon}^{-1}$; water usage by rice and maize crops were responsible for 40% and 37%
233 of this value, respectively. In January and February of each year, the $WFCP_g$ comprised almost 75% of the monthly WFCP.
234 The annual peak of the $WFCP_g$ alternated between June and July, with an average annual value of $83 \text{ Gm}^3 \text{ mon}^{-1}$, 40% of which
235 was attributable to water consumption by maize crops. The monthly WFCP values revealed that the peaks of evaporation
236 (average annual value of $45 \text{ Gm}^3 \text{ mon}^{-1}$) and transpiration (average annual value of $56 \text{ Gm}^3 \text{ mon}^{-1}$) for the 21 crops occurred
237 in May and July, respectively (Fig. S2 and S3). The monthly WFCP fluctuated within each crop; nevertheless, the relative
238 contributions of evapotranspiration and transpiration to total water consumption during the same growth period varied less
239 from year to year. The above analysis allowed us to identify the quantity, type, and periods of water consumption by each crop.

240 The grid-scale spatial distributions of the monthly WFCP, $WFCP_b$, and $WFCP_g$ values are shown in Fig. 3. The months
241 with large grid WFCP ($WFCP > 50 \text{ mm mon}^{-1}$, $WFCP_b > 10 \text{ mm mon}^{-1}$, and $WFCP_g > 30 \text{ mm mon}^{-1}$) mainly comprised April
242 to August. The Northeast Plain, North Plain, and Sichuan Basin contained the regions with the highest grid WFCP. The grid
243 WFCP varied considerably among the 21 crops, but its spatial distribution was consistent within the planted area of each crop.
244 In addition, the regional distribution of grid $WFCP_b$ and $WFCP_g$ values of each crop exhibited significant spatial heterogeneity
245 (Fig. S4 and S5). The grid WFCP, $WFCP_b$, and $WFCP_g$ of sprinkler irrigation at the monthly and annual scales were
246 significantly higher than those of the other two irrigation practices, and high-value regions were concentrated in the northeast,
247 southwest, and south of China (Fig. S6–S10). The relative blue and green water consumption via evaporation and transpiration
248 depended on the natural conditions prevailing at the time and in the space where the 21 crops were grown, as well as the water
249 supply modes and irrigation practices (Fig. S11–S14).

250



251

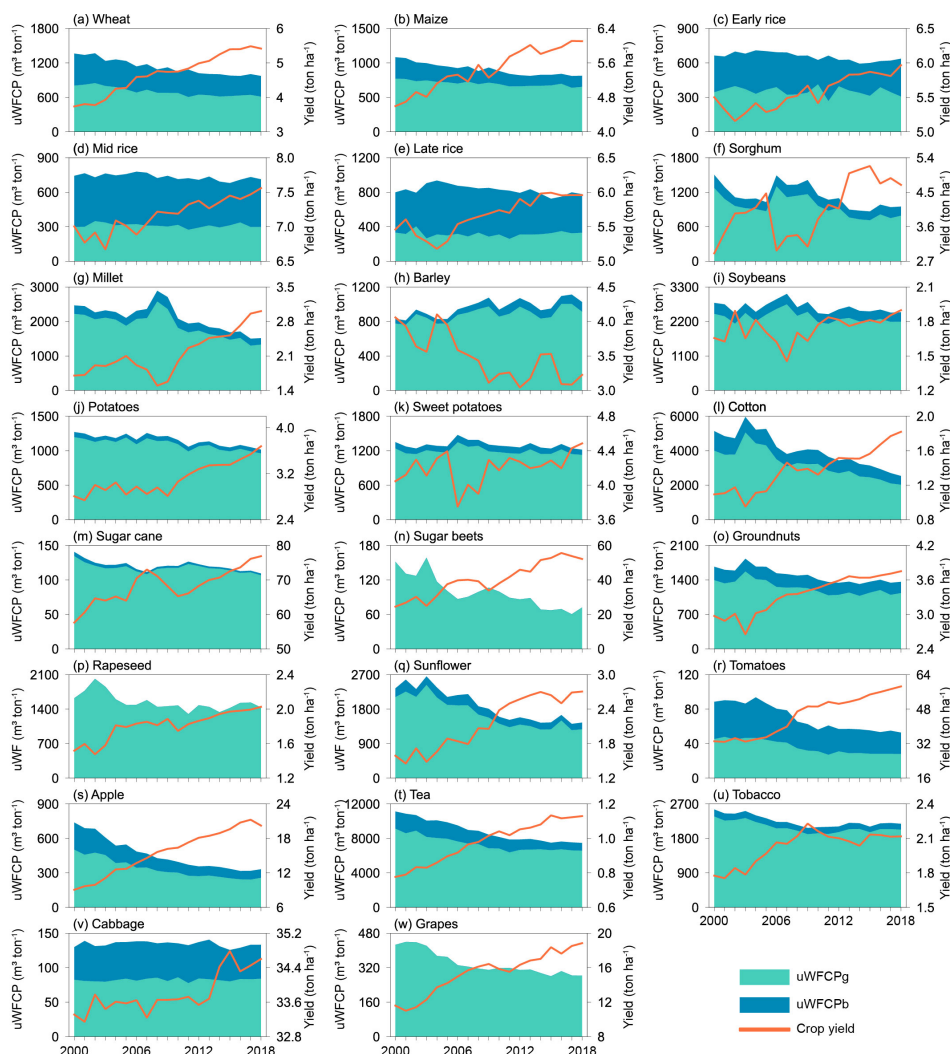
252 **Figure 3.** Gridded monthly total WFCP (a), WFCPb (b), and WFCPg (c) of 21 crops in China by 2017.



253 **3.2 Water footprint per unit of crop production**

254 Tea ($8372 \text{ m}^3 \text{ ton}^{-1}$), cotton ($3974 \text{ m}^3 \text{ ton}^{-1}$), and tobacco ($2242 \text{ m}^3 \text{ ton}^{-1}$) had comparatively large uWFCP, whereas fruits
 255 and vegetables had a uWFCP of less than $500 \text{ m}^3 \text{ ton}^{-1}$. Among the grain crops, wheat and maize had uWFCP of $1110 \text{ m}^3 \text{ ton}^{-1}$
 256 ¹ and $883 \text{ m}^3 \text{ ton}^{-1}$, respectively. Late rice ($826 \text{ m}^3 \text{ ton}^{-1}$) had a slightly greater uWFCP than early ($654 \text{ m}^3 \text{ ton}^{-1}$) and mid (732
 257 $\text{m}^3 \text{ ton}^{-1}$) rice. The uWFCP, uWFCP_b, and uWFCP_g for all 21 crops showed a trend of fluctuating decline during the study
 258 period as yield grew (Fig. 4). The uWFCP of cotton (51%), sugar beets (52%), and apple (55%) showed the greatest reduction.
 259 The uWFCP of wheat and maize decreased by more than 25%, because the yield increased by 45% and 33%, respectively.

260



261
 262

Figure 4. Interannual variation in uWFCPb, uWFCPg, and yield of 21 crops in China over 2000-2018.



263 The uWFCP of the 21 crops was relatively high under rain-fed conditions (Table 4, Fig. S15). Additionally, the uWFCP_b,
 264 uWFCP_g, and yield of each crop responded differently to the three irrigation treatments. These variations were caused by the
 265 fact that the proportions of blue and green water consumption via soil evaporation and crop transpiration differed between
 266 crops and irrigation practices (Fig. S16). For example, blue water consumption via crop transpiration in furrow and sprinkler
 267 irrigation accounted for 45% and 51% of the total crop water consumption, respectively, which was much lower than that of
 268 micro-irrigation (62%). Therefore, the effects of different water supply modes and irrigation practices should be considered in
 269 the quantification of uWFCP over a long time series.

270

271 **Table 4. The uWFCP_b, uWFCP_g, and yield of 21 crops under different water supply modes and irrigation practices.**

Crop	Furrow irrigation			Micro irrigation			Sprinkler irrigation			Rain-fed	
	Blue uWFCP m ³ ton ⁻¹ (Δ)	Green uWFCP m ³ ton ⁻¹ (Δ)	Yield ton ha ⁻¹ (Δ)	Blue uWFCP m ³ ton ⁻¹ (Δ)	Green uWFCP m ³ ton ⁻¹ (Δ)	Yield ton ha ⁻¹ (Δ)	Blue uWFCP m ³ ton ⁻¹ (Δ)	Green uWFCP m ³ ton ⁻¹ (Δ)	Yield ton ha ⁻¹ (Δ)	Green uWFCP m ³ ton ⁻¹ (Δ)	Yield ton ha ⁻¹ (Δ)
Wheat	508 (-30%)	447 (-18%)	6.1 (36%)	628 (-18%)	340 (-29%)	5.1 (20%)	636 (-31%)	464 (-16%)	5.5 (35%)	999 (-38%)	4.5 (80%)
Maize	369 (-26%)	477 (-15%)	6.4 (25%)	369 (-26%)	238 (-52%)	9.4 (80%)	390 (-38%)	396 (-24%)	7.3 (39%)	820 (-26%)	5.7 (43%)
Early rice	231 (4%)	406 (-6%)	0.2 (463%)	–	–	–	332 (4%)	305 (-12%)	172.6 (-79%)	–	–
Mid rice	349 (-24%)	382 (-4%)	0.6 (361%)	–	–	–	420 (-5%)	291 (-2%)	91.7 (-73%)	–	–
Late rice	237 (8%)	540 (-2%)	0.2 (526%)	–	–	–	454 (-3%)	322 (-2%)	156.6 (-81%)	–	–
Sorghum	601 (-43%)	793 (-29%)	3.7 (54%)	713 (-21%)	567 (-42%)	3.8 (52%)	693 (-56%)	696 (-39%)	3.9 (82%)	805 (-39%)	5.2 (67%)
Millet	719 (-45%)	807 (-32%)	3.5 (65%)	705 (-36%)	531 (-47%)	3.8 (68%)	712 (-51%)	652 (-38%)	4.0 (76%)	1,528 (-38%)	2.8 (75%)
Barley	369 (15%)	536 (15%)	3.7 (-7%)	660 (86%)	558 (55%)	2.9 (-26%)	1,038 (117%)	1,069 (130%)	2.1 (-48%)	1,051 (25%)	3.1 (-24%)
Soybeans	915 (-14%)	1,569 (-8%)	2.2 (12%)	1,359 (-1%)	1,236 (-19%)	2.1 (14%)	1,006 (-29%)	1,575 (6%)	2.0 (2%)	2,489 (-11%)	1.8 (16%)
Potatoes	192 (-10%)	258 (25%)	9.9 (-22%)	188 (-14%)	105 (-30%)	19.0 (31%)	156 (-3%)	150 (42%)	17.0 (-24%)	1,253 (-28%)	2.9 (47%)
Sweet potatoes	403 (-26%)	762 (-7%)	5.1 (14%)	485 (-22%)	751 (-3%)	4.9 (11%)	457 (-38%)	721 (4%)	5.2 (9%)	1,231 (-8%)	4.3 (10%)
Cotton	2,539 (-18%)	2,623 (-3%)	1.4 (17%)	1,306 (-53%)	360 (-80%)	4.5 (208%)	2,807 (-22%)	2,704 (20%)	1.3 (3%)	2,133 (-55%)	1.8 (71%)
Sugar cane	16 (-31%)	37 (-32%)	164.9 (56%)	13 (-10%)	29 (-17%)	200.7 (26%)	19 (-43%)	41 (-41%)	146.1 (83%)	120 (-26%)	69.8 (40%)
Sugar beets	8 (-35%)	2 (-36%)	752.3 (54%)	7 (-35%)	2 (-32%)	786.0 (49%)	10 (-26%)	4 (-23%)	520.9 (30%)	72 (-53%)	52.2 (114%)
Groundnuts	440 (-35%)	608 (-29%)	5.5 (50%)	633 (0%)	540 (-10%)	5.0 (11%)	534 (-41%)	567 (-14%)	5.5 (32%)	1,669 (-5%)	2.8 (8%)
Rapeseed	181 (35%)	611 (-48%)	6.0 (58%)	116 (19%)	676 (-39%)	6.0 (52%)	181 (35%)	611 (-48%)	6.0 (58%)	1,435 (-12%)	2.0 (34%)



Sunflower	829	639	3.6	694	250	6.0	794	485	4.5	1,504	2.4
	(-27%)	(-6%)	(21%)	(-42%)	(-62%)	(121%)	(-30%)	(-13%)	(28%)	(-39%)	(72%)
Tomatoes	25	28	58.6	28	22	58.7	27	25	58.6	–	–
	(-43%)	(-38%)	(77%)	(-41%)	(-39%)	(77%)	(-52%)	(-31%)	(77%)	–	–
Apple	159	150	26.1	200	128	20.9	219	177	21.1	345	17.5
	(-65%)	(-56%)	(159%)	(-40%)	(-54%)	(87%)	(-66%)	(-55%)	(151%)	(-48%)	(111%)
Tea	1,769	2,552	2.3	1,546	2,601	2.2	1,620	2,218	2.6	10,769	0.7
	(-52%)	(-57%)	(138%)	(-64%)	(-66%)	(221%)	(-65%)	(-63%)	(198%)	(-17%)	(17%)
Tobacco	596	1,303	2.6	486	1,436	2.2	622	1,110	2.9	2,281	2.0
	(-25%)	(-5%)	(13%)	(-24%)	(13%)	(-14%)	(-40%)	(9%)	(6%)	(-15%)	(20%)
Cabbage	49	85	34.7	53	71	32.7	48	79	35.0	–	–
	(4%)	(2%)	(4%)	(6%)	(-7%)	(-2%)	(-14%)	(9%)	(5%)	–	–
Grapes	135	63	33.8	115	54	33.8	148	64	33.8	283	18.8
	(-44%)	(-45%)	(80%)	(-45%)	(-46%)	(80%)	(-44%)	(-45%)	(80%)	(-34%)	(63%)

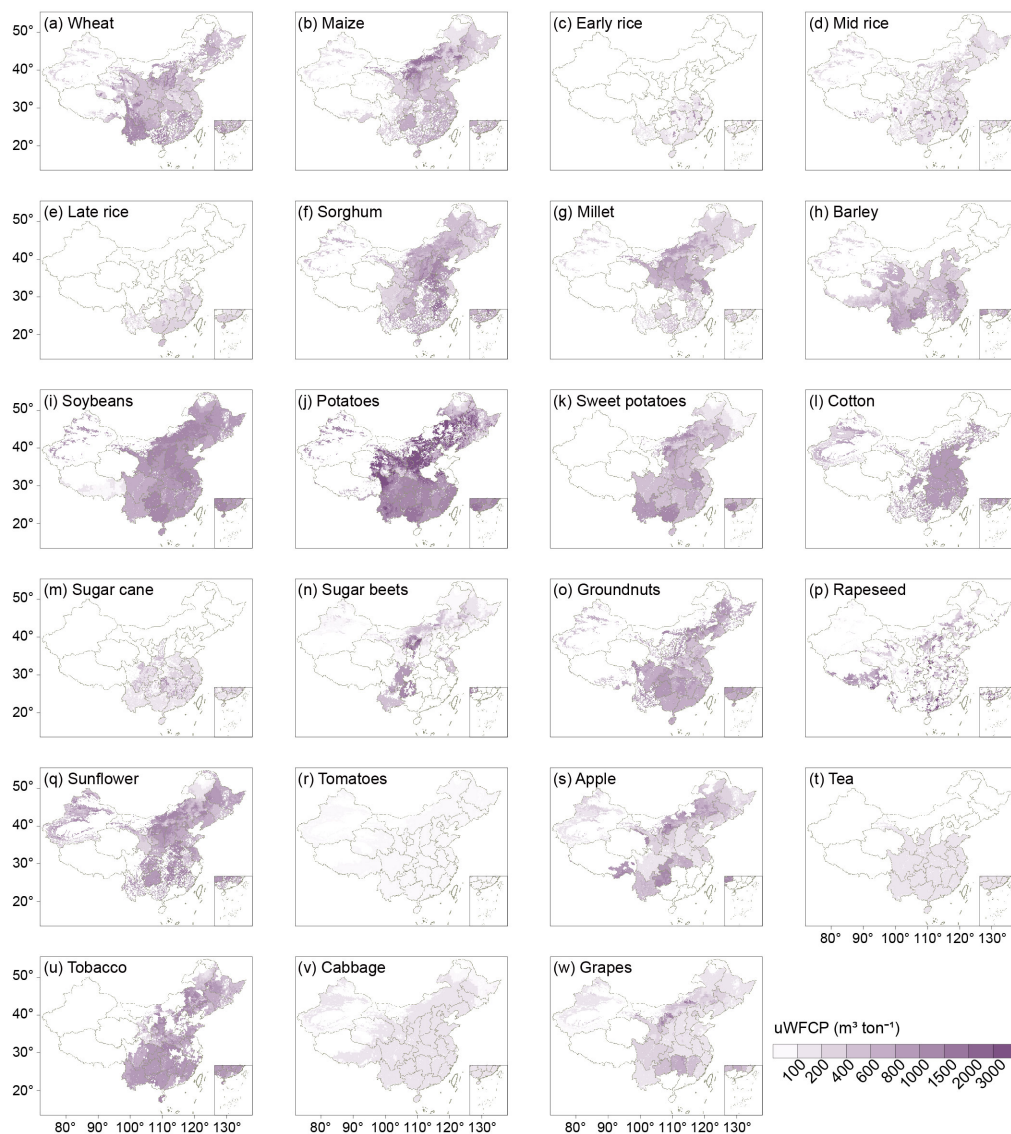
272 Note: “△” refers to the rate of change from 2000 to 2018. “-” indicates that no crops are grown.

273

274 The spatial distribution of the gridded uWFCP showed significantly heterogeneity (Fig. 5, S17, and S18). There were
 275 many regions with high-gridded uWFCP values for potatoes, which were concentrated in northern China. The crop with the
 276 densest distribution of high-gridded uWFCP_b values was tea, which was commonly dispersed throughout the southern regions.
 277 Soybean and millet possessed more uWFCP_g high-value areas, mainly in the northern regions. By comparing the relative
 278 changes in the average grid uWFCP from the period of 2000–2009 to that of 2010–2018, it was determined that the uWFCP of
 279 all 21 crops exhibited a spatially significant decreasing trend (Fig. S19–S21). It is essential to emphasise that the dominant
 280 factors governing this decrease in uWFCP varied among crops. For example, the decline observed in the uWFCP of apple was
 281 attributable to a substantially larger decrease in uWFCP_g than the corresponding rise in uWFCP_b, whereas that observed for
 282 tea was caused by a considerable decrease in uWFCP_b.

283 For most crops, rainfed ones had more regions of high uWFCP than irrigated ones, and the geographical distribution of
 284 uWFCP for the same crop was generally consistent, regardless of irrigation practices. The variation in uWFCP_b and uWFCP_g
 285 for the same water supply mode and irrigation practice in a crop was considerable owing to regional water consumption and
 286 yield differences (Fig. S22 and S23). Additionally, the temporal evolution of uWFCP_b and uWFCP_g under various water supply
 287 modes and irrigation practices was analysed, and rainfed crops demonstrated a more rapid and wider reduction in uWFCP than
 288 irrigated crops.

289



290

291 **Figure 5. Gridded uWFCP of 21 crops in China at annual average level for 2000-2018.**

292

293 3.3 Benchmarks for uWFCP

294

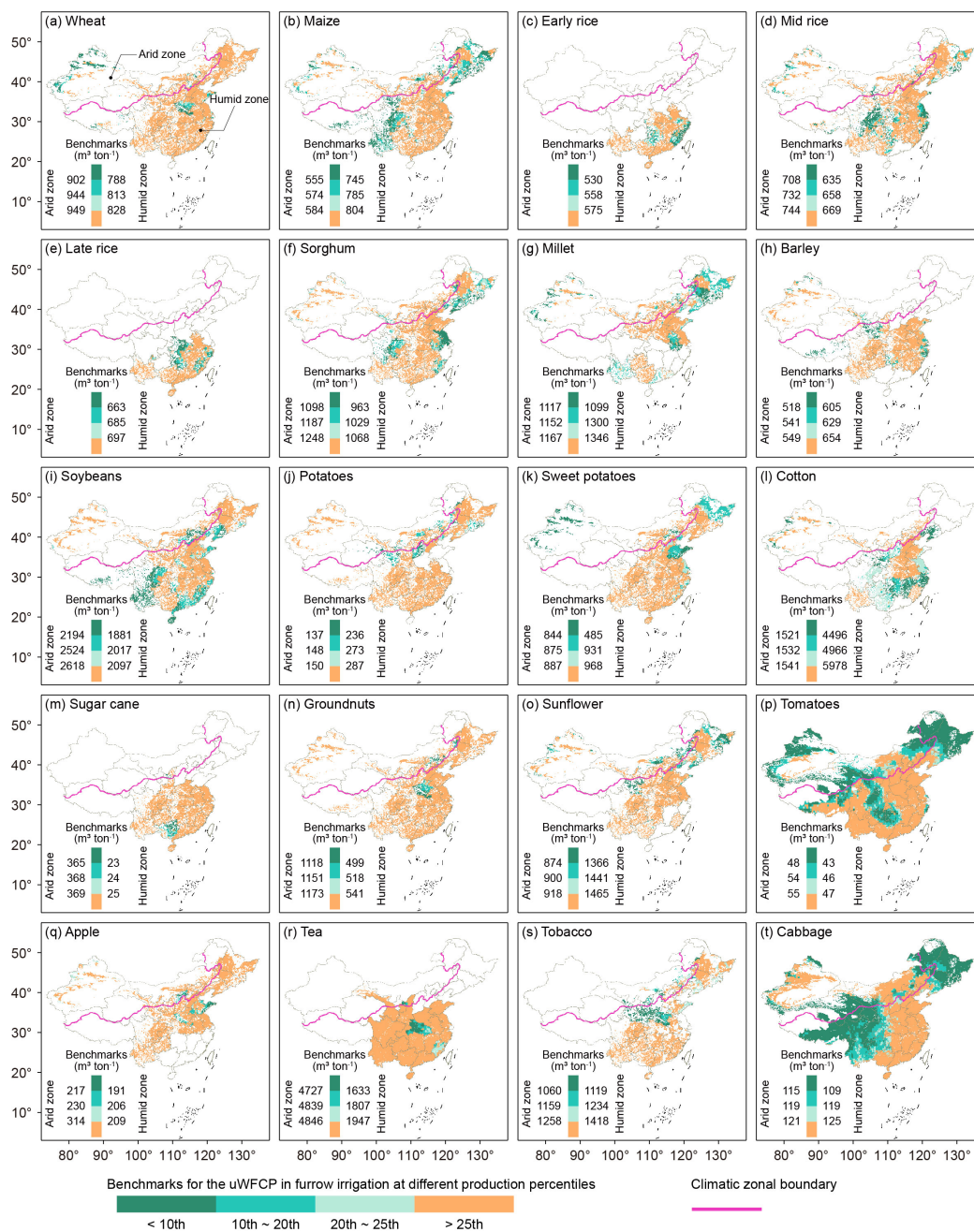
Annual uWFCP benchmarks were calculated using the different production percentiles for each of the 21 crops under
295 various water supply modes and irrigation practices (Table S1). Significant interannual differences existed between these
296 uWFCP benchmarks; therefore, it will be necessary to reassess these benchmarks using longer time-series measurements to
297 reduce the impact of years with exceptional results as outliers in the dataset. The benchmarks for the uWFCP of different crops



298 responded differently to climatic zone. Crops such as millet, soybeans, and groundnuts had higher benchmarks for uWFCP in
299 arid zones than in humid zones due to differences in production percentiles; the reverse was true for maize, cotton, and
300 sunflower. Overall, the uWFCP benchmarks for rainfed crops were higher than those for irrigated crops. The uWFCP
301 benchmarks for each irrigation practice varied by crop species.

302 Fig. 6 and Fig. S26–S28 present the uWFCP benchmarks according to different production percentiles in humid and arid
303 zones and as obtained for various water supply modes and irrigation practices. Except for vegetables (tomatoes and cabbage),
304 the majority of crops were cultivated in regions with a uWFCP benchmark that exceeded the 25% production percentile. Under
305 furrow and sprinkler irrigation, the areas that fell below the uWFCP benchmark at the 25% production percentile were
306 predominantly distributed in the humid zone. In the arid zone, a greater proportion of micro-irrigated regions fell below the
307 uWFCP benchmark at the 25% production percentile. The results indicate that governing bodies need to consider the influence
308 of climatic zones as well as water supply modes and irrigation practices when quantifying uWFCP benchmarks to identify
309 hotspots for water-saving potential; specific water-use policies need to be formulated both for crop varieties and irrigation
310 practices.

311



312

313 **Figure 6. Benchmarks for uWFCP at different production percentiles under furrow irrigation in China by 2018.**

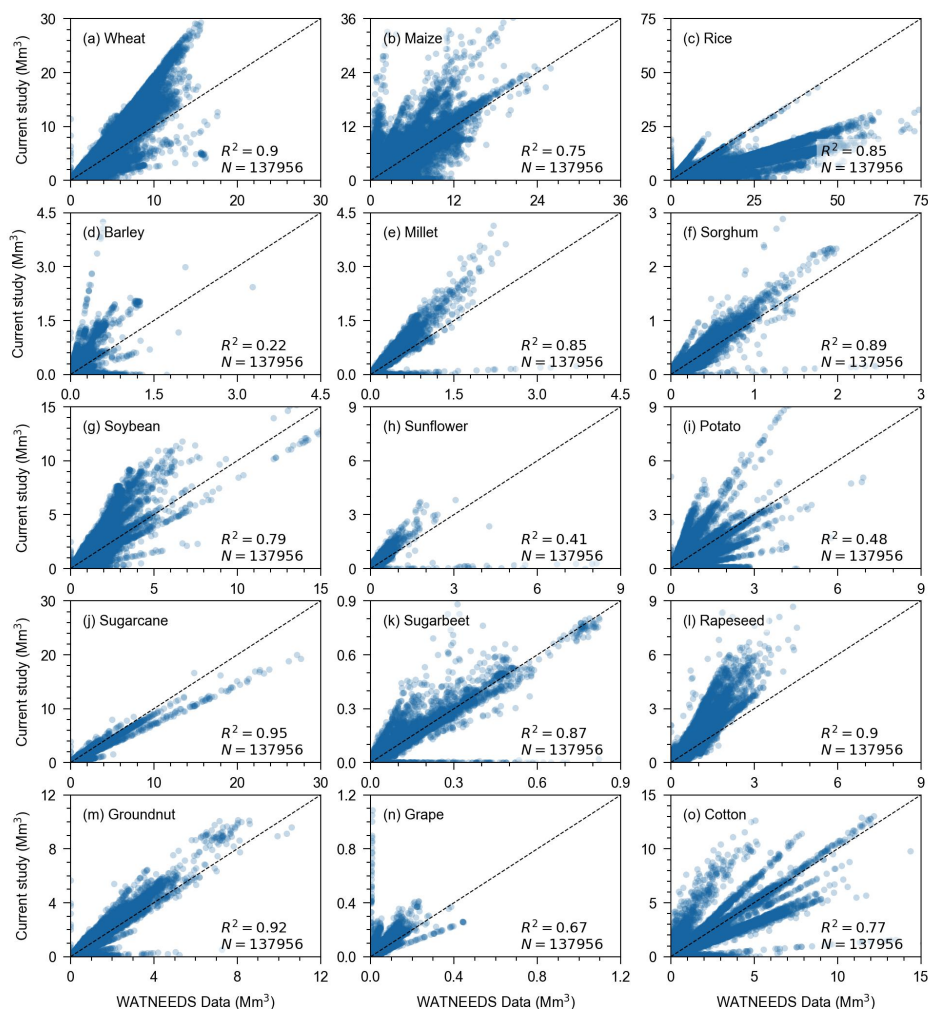
314



315 **3.4 Results comparison**

316 Using publicly available datasets, we compared the water use of 15 crops with the WATNEEDS dataset (Chiarelli et al.,
317 2020) that overlapped in time (in 2000) and space (137,956 grids). As illustrated in Fig. 7, the results showed that $R^2 > 0.60$ (p
318 < 0.01) among 12 of the crops. However, large deviations were present in the comparisons of data for barley, sunflower, and
319 potatoes. The following two factors were responsible for this disparity. First, the current study aimed to quantify the actual
320 water consumption during crop growth, whereas the WATNEEDS dataset concentrated on theoretical crop water requirements.
321 Second, this study divided irrigation into furrow, sprinkler, and micro-irrigation categories at the grid scale. In reality, sprinkler
322 irrigation covers a much larger area than micro-irrigation does and also possesses the highest f_w of our three irrigation categories,
323 which is ultimately reflected in a higher water consumption in our data. Overall, our dataset displayed a high level of reliability.
324 The comparison of our WFCP data with the WATNEEDS dataset (Chiarelli et al., 2020) on a national scale is shown in Table
325 5. Except for rice, the variability of WFCP and WFCP_b between the two datasets was under 25% and 20%, respectively,
326 demonstrating high consistency. Large differences in the WFCP_g between the two datasets can be attributed to two factors,
327 namely, the different quantification methods used (including model mechanisms and green water definitions) and the different
328 sources of precipitation data used for model input, leading to variations in green water simulations. With regards to the
329 variability observed in rice data, some of our grids contained information for two to three seasons of rice cultivation (combined
330 with the actual regional cultivation), and all of these instances were assumed to receive irrigation in this study; this may have
331 resulted in a comparatively low WFCP_g value.

332



333

334 **Figure 7. Comparison of WFCP with WATNEEDS dataset.**

335

336 In a comparison of the uWFCP obtained for 21 crops in our dataset with figures reported by Mekonnen and Hoekstra
337 (2011) and Zhuo et al. (2016a), the variability of data for 18 crops was under 30%, which was attributed to the uncertainty
338 imposed by model simulation (Table 5). Although crop acreage remains consistent at the national scale, sets of crop distribution
339 data must be matched with different sets of input variables (such as precipitation, temperature, and soil moisture content),
340 which has a significant impact on the simulated values. The differences in the uWFCP of potato, sweet potato, and cotton
341 resulted from the large discrepancies in production data, with simulated values for these three crops by Mekonnen and Hoekstra
342 (2011) and Zhuo et al. (2016a) being 80%, 81%, and 67% higher than the statistical yearbook.

343



344 **Table 5. Comparison of WFCP and uWFCP in overlapping time and space with published results.**

Crop	WFCP					uWFCP					uWFCP				
	Unit: M m ³ yr ⁻¹ . Period: 2000.					Unit: m ³ ton ⁻¹ . Period: 2000-2005.					Unit: m ³ ton ⁻¹ . Period: 2000-2009.				
	Current study		Chiarelli et al., 2020		(Δ)	Current study		Mekonnen and Hoekstra, 2011		(Δ)	Current study		Zhuo et al., 2016a		(Δ)
	Blue	Green	Blue	Green		Blue	Green	Blue	Green		Blue	Green	Blue	Green	
Wheat	80	55	79	22	(14%)	800	501	821	466	(1%)	754	472	1,135	392	(11%)
Maize	82	33	78	24	(6%)	744	264	791	74	(8%)	728	239	747	56	(9%)
Rice	59	80	255	97	(43%)	328	432	549	246	(2%)	323	437	987	395	(29%)
Sorghum	3	1	3	0	(4%)	1,002	178	952	42	(9%)	1,059	186	695	58	(25%)
Millet	5	1	4	0	(11%)	2,092	224	1,600	40	(17%)	2,145	242	1,418	141	(21%)
Barley	3	0	4	0	(21%)	804	50	556	28	(19%)	843	58	560	120	(14%)
Soybeans	38	5	33	5	(5%)	2,337	326	2,549	249	(2%)	2,418	317	2,336	316	(2%)
Potatoes	16	1	16	1	(0%)	1,163	62	215	7	(69%)	1,154	64	183	9	(73%)
Sweet potatoes	29	3				1,184	105	242	4	(68%)	1,211	108	63	22	(88%)
Cotton	18	5	23	3	(8%)	4,236	951	1,440	247	(51%)	3,781	847	1,117	281	(54%)
Sugar cane	9	0	12	1	(17%)	122	5	169	6	(16%)	118	4	124	1	(1%)
Sugar beets	1	0	1	0	(2%)	130	0	148	0	(6%)	117	0	104	0	(6%)
Groundnuts	20	4	19	3	(5%)	1,412	257	1,383	85	(6%)	1,347	260	1,399	219	(0%)
Rapeseed	18	0	12	0	(22%)	1,713	0	1,387	0	(11%)	1,623	0	1,754	0	(4%)
Sunflower	4	0	3	0	(9%)	2,154	232	2,254	341	(4%)	1,991	237	1,025	163	(30%)
Tomatoes	1	1				46	43	182	3	(35%)	42	39	81	2	(2%)
Apple	10	5				443	186	796	30	(14%)	389	154	372	46	(13%)
Tea	6	1				8,440	1,970	9,277	798	(2%)	7,860	1,792	9,055	122	(3%)
Tobacco	6	0				2,273	174	2,007	253	(4%)	2,162	167	1,771	18	(13%)
Cabbage	3	2				82	53	237	4	(28%)	82	53	122	8	(2%)
Grapes	1	0	1	0	(7%)	407	0	357	0	(7%)	364	0	349	123	(13%)

345 Note: “ Δ ” Calculated as the ratio of the study difference to the study mean.

346

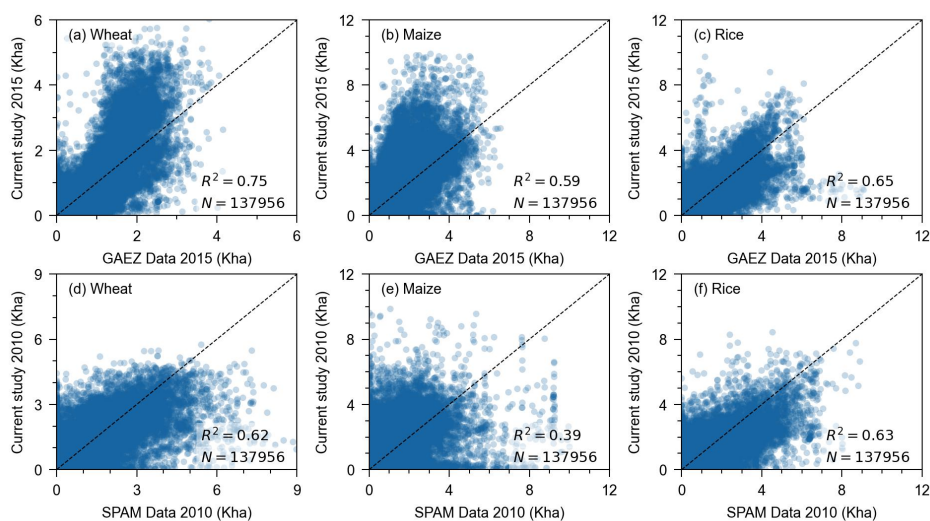
347 4 Discussion

348 4.1 Data validation

349 We compared our 5 arcmin resolution of major crop areas between 2001 and 2018, as calculated by the proportional
 350 invariant method, with the GAEZ+2015 (Grogan et al., 2022) and MapSPAM2010 (IFPRI, 2019) data products (Fig. 8). Linear
 351 regression results for data on wheat, maize, and rice coverage showed that R^2 was greater than 0.50 ($p < 0.01$) at the raster
 352 scale and greater than 0.80 ($p < 0.01$) at the provincial scale, and the overall variability at the national scale was under 8%.

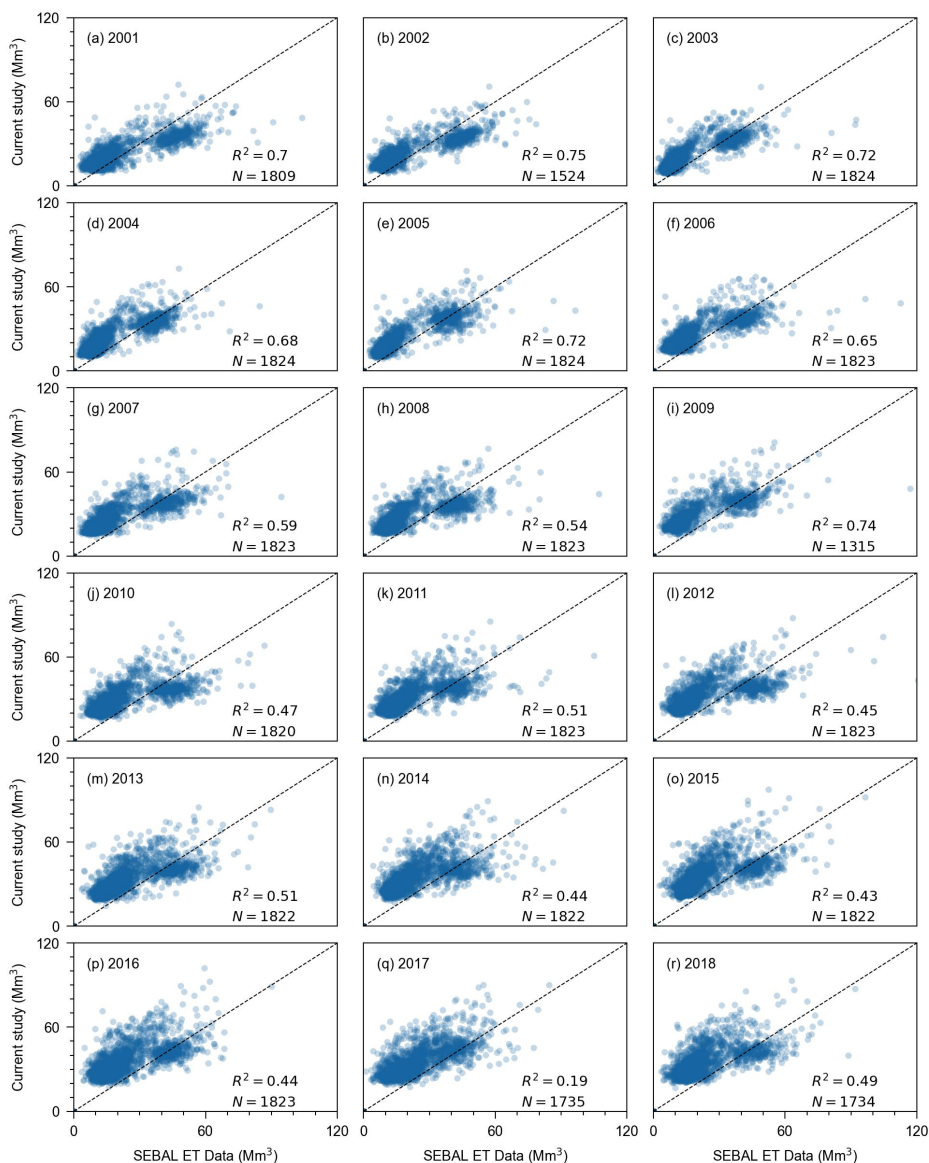


353 Overall, comparisons with existing products validated the accuracy of the gridded representation of crop land coverage as
354 obtained in this study.
355



356
357 **Figure 8. Comparison of the current gridded area representing land coverage by major crops with the GAEZ+2015 and**
358 **MapSPAM2010 datasets.**

359
360 Based on data from remote sensing products, we validated our evapotranspiration data (Fig. 9) by following the selection
361 process outlined in Section 2.3.2. Our evapotranspiration results were higher than the SEBAL product (Cheng et al., 2021),
362 which is a daily time series evapotranspiration product based on MOD16 data, but had good overall consistency ($R^2 > 0.50$, p
363 < 0.01) for 11 out of the 18 years. The reality of interannual variability in agricultural practices (irrigation vs. non-irrigation)
364 and the presence of deficit irrigation could result in the low evapotranspiration data of remote sensing products relative to that
365 generated in model simulations. In general, a comparison of our dataset with those of SEBAL product verified the accuracy of
366 our model.
367



368

369 **Figure 9. Validation of the evapotranspiration at croplands with SEBAL datasets.**

370

371 **4.2 Sensitivity and uncertainty analysis**

372 To clarify the sensitivity of a WFCP assessment to the main parameters in a simulation, a previous study by the authors
373 applied the one-at-a-time and sensitivity index methods to quantitatively evaluate a WFCP calculation by AquaCrop (Li et al.,
374 2022). The results indicated that crop water consumption and production were extremely sensitive to the reference



375 evapotranspiration and the crop transpiration coefficient. The soil evaporation coefficient furthermore influenced soil
376 evaporation in the root zone, and consequently, WFCP. The effect of planting date differed for each crop, and advancing or
377 delaying it exposed crops to completely different rain and heat conditions. Importantly, the accuracy of all model studies
378 (including those using AquaCrop) is dependent on both the model mechanism and the input data. AquaCrop's accuracy in
379 simulating crop water consumption and production for various climates, soils, and field management practices has been
380 extensively validated (Zhuo et al., 2016a; Pirmoradian and Davatgar, 2019; Wang et al., 2019; Chibarabada et al., 2020).

381 At the outset of the simulation used in this study, we rigorously screened the input data according to the principles of
382 accuracy and representativeness. However, there was a degree of bias in the model setup and input data. For instance, the
383 current study focused on the effect of water stress on crop growth and worked from the assumption that all nutrients required
384 for crops were provided. AquaCrop, as a water-driven model, simulates crop growth comprehensively by establishing the
385 responsive link between effective soil water usage and crop yield (Raes et al., 2018). However, there is a serious
386 overapplication of chemical fertilisers in Chinese farmlands (Chen et al., 2014; Cui and Shoemaker, 2018). Furthermore, the
387 parameters we used for fraction of the surface wetted in either furrow, sprinkler, or micro-irrigation remained consistent across
388 regions owing to the absence of any data related to possible variance; in other words, we downplayed regional variations within
389 the same irrigation practice. Taking micro-irrigation as an example, the difference between different micro-irrigation products
390 mostly lies in the transport and distribution pipe networks and irrigator, which have little impact on the fraction of the surface
391 wetted in the crop root zone. In terms of crop parameters, we set many constant parameters for the same crops that do not vary
392 with simulation time and space, including planting date, harvest date, harvest index, and root depth, which will also lead to
393 inaccurate assessments of crop production and water consumption (Waha et al., 2012). Consequently, in future research,
394 attention to the collection and organisation of basic data can play a positive role in the improvement of the model mechanism
395 and accuracy of the output (Mekonnen and Hoekstra, 2010; Mekonnen and Hoekstra, 2011).

396 In general, despite the uncertainties in the input data, the calculated WFCP and uWFCP were in good agreement with
397 existing studies at both the grid and national scales, and the dataset in the long time series was compatible with remote sensing
398 products. The above analysis demonstrated that the findings of our current study correctly reflected water consumption during
399 the crop growth period under various water supply modes and irrigation practices.

400 **5 Data availability**

401 All data used in this study are freely available with the links given in Sect. 2. The dataset presented in this article are
402 available from the Zenodo repository at <https://doi.org/10.5281/zenodo.7756013> (Wang et al., 2023). Both gridded



403 consumptive water footprints, evaporation, transpiration, and associate benchmarks of crop production are provided.

404 **6 Conclusions**

405 The current study constructed a gridded WFCP database for 21 crops in China for 2000-2018 to reflect different water
406 supply modes and irrigation practices, thereby addressing monthly blue and green water consumption in soil evaporation and
407 crop transpiration. Additionally, we established uWFCP benchmarks for various climatic zones, water supply modes and
408 irrigation practices. The current dataset was thoroughly validated. The results highlighted the necessity to explore the
409 influences of different field management practices on WFCP quantification and benchmarking in future research.

410 The WFCP is a crucial indicator used for evaluating water consumption by crops and a key component to solving the
411 problems associated with the environmental "footprint family" and "planetary boundary" (Galli et al., 2012; Hoekstra and
412 Wiedmann, 2014; Steffen et al., 2015). The current dataset is able to support for precise crop water productivity assessments,
413 agricultural water-saving evaluations, the development of sustainable irrigation techniques, cropping structure optimisation,
414 and crop-related interregional virtual water trade analysis. The dataset can furthermore be applied to develop dynamic water
415 management policies by virtue of its analysis of the spatial and temporal fluctuations in crop water consumption. The
416 methodological framework for batch quantification of the WFCP can facilitate the updating of relative dataset and scale
417 conversion studies.

418 **Author contributions**

419 LZ and PW designed the research. WW collected basic data, performed simulations, and conducted results validation and
420 calibration. XJ conducted the sensitivity analysis. ZY, ZL, ML, HZ, RG, CY, and PZ performed simulations. WW and LZ
421 wrote the original manuscript. LZ and PW revised the manuscript.

422 **Competing interests**

423 The contact author has declared that neither they nor their co-authors have any competing interests.

424 **Acknowledgements**

425 We thank all colleagues for their support and work. The dataset could not be established without the contributions of all
426 participants.



427 **Financial support**

428 The study is financially supported by the Program for Cultivating Outstanding Talents on Agriculture, Ministry of
429 Agriculture and Rural Affairs, People's Republic of China (13210321), and the National Youth Talents Plan, and Chinese
430 Universities Scientific Fund (2452021168) to LZ.

431 **References**

- 432 Allen, R. G., Pereira, L. S., Raes, D., and Smith, M.: Crop evapotranspiration—Guidelines for computing crop water
433 requirements-FAO Irrigation and drainage paper 56, 300, D05109, FAO, Rome, 1998.
- 434 Batjes, N. H.: ISRIC-WISE derived soil properties on a 5 by 5 arc-minutes global grid (ver. 1.2), ISRIC-World Soil Information,
435 available at: [https://data.isric.org/geonetwerk/srv/eng/catalog.search#/metadata/82f3d6b0-a045-4fe2-b960-](https://data.isric.org/geonetwerk/srv/eng/catalog.search#/metadata/82f3d6b0-a045-4fe2-b960-6d05bc1f37c0)
436 [6d05bc1f37c0](https://data.isric.org/geonetwerk/srv/eng/catalog.search#/metadata/82f3d6b0-a045-4fe2-b960-6d05bc1f37c0). (last access: 7 March 2023), 2012.
- 437 Brown, J. F. and Pervez, M. S.: Merging remote sensing data and national agricultural statistics to model change in irrigated
438 agriculture, *Agric. Syst.*, 127, 28-40, <https://doi.org/10.1016/j.agsy.2014.01.004>, 2014.
- 439 Chen, X., Cui, Z., Fan, M., Vitousek, P., Zhao, M., Ma, W., Wang, Z., Zhang, W., Yan, X., and Yang, J.: Producing more grain
440 with lower environmental costs, *Nature*, 514, 486-489, <https://doi.org/10.1038/nature13609>, 2014.
- 441 Chen, Y., Guo, G., Wang, G., Kang, S., Luo, H., and Zhang, D.: Main crop water requirement and irrigation of China, Hydraulic
442 and Electric Press, Beijing, 1995.
- 443 Cheng, M., Jiao, X., Li, B., Yu, X., Shao, M., and Jin, X.: Long time series of daily evapotranspiration in China based on the
444 SEBAL model and multisource images and validation, *Earth Syst. Sci. Data*, 13, 3995-4017, [https://doi.org/10.5194/essd-](https://doi.org/10.5194/essd-13-3995-2021)
445 [13-3995-2021](https://doi.org/10.5194/essd-13-3995-2021), 2021.
- 446 Chiarelli, D. D., Passera, C., Rosa, L., Davis, K. F., D'Odorico, P., and Rulli, M. C.: The green and blue crop water requirement
447 WATNEEDS model and its global gridded outputs, *Sci. Data*, 7, 273, <https://doi.org/10.1038/s41597-020-00612-0>, 2020.
- 448 Chibarabada, T., Modi, A., and Mabhaudhi, T.: Calibration and evaluation of aquacrop for groundnut (*Arachis hypogaea*) under
449 water deficit conditions, *Agric. For. Meteorol.*, 281, 107850, <https://doi.org/10.1016/j.agrformet.2019.107850>, 2020.
- 450 CAMIYC, China Agricultural Machinery Industry Yearbook Committee: China Agricultural Machinery Industry Yearbook,
451 China Machine Press, Beijing, 2022.
- 452 Chukalla, A. D., Krol, M. S., and Hoekstra, A. Y.: Green and blue water footprint reduction in irrigated agriculture: effect of
453 irrigation techniques, irrigation strategies and mulching, *Hydrol. Earth Syst. Sci.*, 19, 4877-4891,
454 <https://doi.org/10.5194/hess-19-4877-2015>, 2015.



- 455 Cui, K. and Shoemaker, S. P.: A look at food security in China, *NPJ Sci. Food.*, 2, 4, <https://doi.org/10.1038/s41538-018-0012->
456 x, 2018.
- 457 Dijkshoorn, K., van Engelen, V., and Huting, J.: Soil and landform properties for LADA partner countries, ISRIC report,
458 available at: <https://data.isric.org/geonetwork/srv/eng/catalog.search#/metadata/2919b1e3-6a79-4162-9d3a->
459 e640a1dc5aef. (last access: 7 March 2023), 2008.
- 460 Döll, P.: Vulnerability to the impact of climate change on renewable groundwater resources: a global-scale assessment, *Environ.*
461 *Res. Lett.*, 4, 035006, <https://doi.org/10.1088/1748-9326/4/3/035006>, 2009.
- 462 Elliott, J., Deryng, D., Müller, C., Frieler, K., Konzmann, M., Gerten, D., Glotter, M., Flörke, M., Wada, Y., and Best, N.:
463 Constraints and potentials of future irrigation water availability on agricultural production under climate change, *Proc.*
464 *Natl. Acad. Sci. U. S. A.*, 111, 3239-3244, <https://doi.org/10.1073/pnas.1222474110>, 2014.
- 465 FAO, Food and Agriculture Organization: The State of Food and Agriculture 2020. Overcoming water challenges in agriculture.
466 Rome. <https://doi.org/10.4060/cb1447en>, 2020.
- 467 FAO, Food and Agriculture Organization: FAOSTAT statistical database, available at:
468 <https://www.fao.org/faostat/en/#data/QCL>. (last access: 7 March 2023), 2023.
- 469 Fader, M., Gerten, D., Thammer, M., Heinke, J., Lotze-Campen, H., Lucht, W., and Cramer, W.: Internal and external green-
470 blue agricultural water footprints of nations, and related water and land savings through trade, *Hydrol. Earth Syst. Sci.*,
471 15, 1641-1660, <https://doi.org/10.5194/hess-15-1641-2011>, 2011.
- 472 Fisher, J. B., Melton, F., Middleton, E., Hain, C., Anderson, M., Allen, R., McCabe, M. F., Hook, S., Baldocchi, D., and
473 Townsend, P. A.: The future of evapotranspiration: Global requirements for ecosystem functioning, carbon and climate
474 feedbacks, agricultural management, and water resources, *Water Resour. Res.*, 53, 2618-2626,
475 <https://doi.org/10.1002/2016WR020175>, 2017.
- 476 Galli, A., Wiedmann, T., Ercin, E., Knoblauch, D., Ewing, B., and Giljum, S.: Integrating ecological, carbon and water footprint
477 into a “footprint family” of indicators: definition and role in tracking human pressure on the planet, *Ecol. Indic.*, 16, 100-
478 112, <https://doi.org/10.1016/j.ecolind.2011.06.017>, 2012.
- 479 Ghose, B.: Food security and food self-sufficiency in China: from past to 2050, *Food Energy Secur.*, 3, 86-95,
480 <https://doi.org/10.1002/fes3.48>, 2014.
- 481 Grogan, D., Frolking, S., Wisser, D., Prusevich, A., and Glidden, S.: Global gridded crop harvested area, production, yield,
482 and monthly physical area data circa 2015, *Sci. Data*, 9, 15, <https://doi.org/10.1038/s41597-021-01115-2>, 2022.
- 483 Haddeland, I., Heinke, J., Biemans, H., Eisner, S., Flörke, M., Hanasaki, N., Konzmann, M., Ludwig, F., Masaki, Y., and
484 Schewe, J.: Global water resources affected by human interventions and climate change, *Proc. Natl. Acad. Sci. U. S. A.*,



- 485 111, 3251-3256, <https://doi.org/10.1073/pnas.1222475110>, 2014.
- 486 Harris, I., Osborn, T. J., Jones, P., and Lister, D.: Version 4 of the CRU TS monthly high-resolution gridded multivariate climate
487 dataset, *Sci. Data*, 7, 109, <https://doi.org/10.1038/s41597-020-0453-3>, 2020.
- 488 Hoekstra, A. Y.: The water footprint of modern consumer society, Routledge, London, 2013.
- 489 Hoekstra, A. Y. and Chapagain, A. K.: Water footprints of nations: water use by people as a function of their consumption
490 pattern, *Water Resour. Manag.*, 21, 35-48, <https://doi.org/10.1007/s11269-006-9039-x>, 2006.
- 491 Hoekstra, A. Y. and Chapagain, A. K.: Globalization of water: Sharing the planet's freshwater resources, Blackwell Publishing,
492 Oxford, 2008.
- 493 Hoekstra, A. Y. and Wiedmann, T. O.: Humanity's unsustainable environmental footprint, *Science*, 344, 1114-1117,
494 <https://doi.org/10.1126/science.1248365>, 2014.
- 495 Hoekstra, A. Y., Chapagain, A. K., Aldaya, M. M., and Mekonnen, M. M.: The water footprint assessment manual: Setting the
496 global standard, Routledge, London, 2011.
- 497 Hoekstra, A.Y. and Mekonnen, M.M.: The water footprint of humanity. *Proc. Natl. Acad. Sci. U. S. A.*, 109, 3232-3237,
498 <https://doi.org/10.1073/pnas.1109936109>, 2012.
- 499 IFPRI, International Food Policy Research Institute: Global spatially-disaggregated crop production statistics data for 2010
500 version 2.0, available at: <https://doi.org/10.7910/DVN/PRFF8V>. (last access: 7 March 2023), 2019.
- 501 IGSNRR, Institute of Geographic Sciences and Natural Resources Research, CAS: Resource and Environment Science and
502 Data Center, available at: <https://www.resdc.cn/data.aspx?DATAID=274>. (last access: 7 March 2023), 2022.
- 503 Jägermeyr, J., Pastor, A., Biemans, H., and Gerten, D.: Reconciling irrigated food production with environmental flows for
504 Sustainable Development Goals implementation, *Nat. Commun.*, 8, 15900, <https://doi.org/10.1038/ncomms15900>, 2017.
- 505 Jung, M., Reichstein, M., Ciais, P., Seneviratne, S. I., Sheffield, J., Goulden, M. L., Bonan, G., Cescatti, A., Chen, J., and De
506 Jeu, R.: Recent decline in the global land evapotranspiration trend due to limited moisture supply, *Nature*, 467, 951-954,
507 <https://doi.org/10.1038/nature09396>, 2010.
- 508 Leng, G., Huang, M., Tang, Q., Gao, H., and Leung, L. R.: Modeling the effects of groundwater-fed irrigation on terrestrial
509 hydrology over the conterminous United States, *J. Hydrometeorol.*, 15, 957-972, [https://doi.org/10.1175/JHM-D-13-](https://doi.org/10.1175/JHM-D-13-049.1)
510 049.1, 2014.
- 511 Li, Z., Feng, B., Wang, W., Yang, X., Wu, P., and Zhuo, L.: Spatial and temporal sensitivity of water footprint assessment in
512 crop production to modelling inputs and parameters, *Agric. Water Manage.*, 271, 107805,
513 <https://doi.org/10.1016/j.agwat.2022.107805>, 2022.
- 514 Lian, X., Piao, S., Huntingford, C., Li, Y., Zeng, Z., Wang, X., Ciais, P., McVicar, T. R., Peng, S., and Otlé, C.: Partitioning



- 515 global land evapotranspiration using CMIP5 models constrained by observations, *Nat. Clim. Chang.*, 8, 640-646,
516 <https://doi.org/10.1038/s41558-018-0207-9>, 2018.
- 517 Liu, J., Williams, J. R., Zehnder, A. J., and Yang, H.: GEPIC—modelling wheat yield and crop water productivity with high
518 resolution on a global scale, *Agric. Syst.*, 94, 478-493, <https://doi.org/10.1016/j.agry.2006.11.019>, 2007.
- 519 Liu, X., Liu, W., Tang, Q., Liu, B., Wada, Y., and Yang, H.: Global agricultural water scarcity assessment incorporating blue
520 and green water availability under future climate change, *Earths Future*, 10, e2021EF002567,
521 <https://doi.org/10.1029/2021EF002567>, 2022.
- 522 Long, D. and Singh, V. P.: Assessing the impact of end-member selection on the accuracy of satellite-based spatial variability
523 models for actual evapotranspiration estimation, *Water Resour. Res.*, 49, 2601-2618, <https://doi.org/10.1002/wrcr.20208>,
524 2013.
- 525 Lovarelli, D., Bacenetti, J., and Fiala, M.: Water Footprint of crop productions: A review, *Sci. Total Environ.*, 548, 236-251,
526 <https://doi.org/10.1016/j.scitotenv.2016.01.022>, 2016.
- 527 Mekonnen, M. M. and Hoekstra, A. Y.: A global and high-resolution assessment of the green, blue and grey water footprint of
528 wheat, *Hydrol. Earth Syst. Sci.*, 14, 1259-1276, <https://doi.org/10.5194/hess-14-1259-2010>, 2010.
- 529 Mekonnen, M. M. and Hoekstra, A. Y.: The green, blue and grey water footprint of crops and derived crop products, *Hydrol.*
530 *Earth Syst. Sci.*, 15, 1577-1600, <https://doi.org/10.5194/hess-15-1577-2011>, 2011.
- 531 Mekonnen, M. M. and Hoekstra, A. Y.: Water footprint benchmarks for crop production: A first global assessment, *Ecol. Indic.*,
532 46, 214-223, <https://doi.org/10.1016/j.ecolind.2014.06.013>, 2014.
- 533 Mialyk, O., Schyns, J. F., Booij, M. J., and Hogeboom, R. J.: Historical simulation of maize water footprints with a new global
534 gridded crop model ACEA, *Hydrol. Earth Syst. Sci.*, 26, 923-940, <https://doi.org/10.5194/hess-26-923-2022>, 2022.
- 535 Middleton, N. and Thomas, D.: *World atlas of desertification: Second Edition*, Arnold, London, 1997.
- 536 NBSC, National Bureau of Statistics: *China Statistical Yearbook*, China Statistical Press, Beijing 2022.
- 537 Pastor, A., Palazzo, A., Havlik, P., Biemans, H., Wada, Y., Obersteiner, M., Kabat, P., and Ludwig, F.: The global nexus of
538 food–trade–water sustaining environmental flows by 2050, *Nat. Sustain.*, 2, 499-507, <https://doi.org/10.1038/s41893-019-0287-1>, 2019.
- 540 Pirmoradian, N. and Davatgar, N.: Simulating the effects of climatic fluctuations on rice irrigation water requirement using
541 AquaCrop, *Agric. Water Manage.*, 213, 97-106, <https://doi.org/10.1016/j.agwat.2018.10.003>, 2019.
- 542 Portmann, F. T., Siebert, S., and Döll, P.: MIRCA2000—Global monthly irrigated and rainfed crop areas around the year 2000:
543 A new high-resolution data set for agricultural and hydrological modeling, *Glob. Biogeochem. Cycle*, 24, GB1011,
544 <https://doi.org/10.1029/2008GB003435>, 2010.



- 545 Puy, A., Lo Piano, S., and Saltelli, A.: Current models underestimate future irrigated areas, *Geophys. Res. Lett.*, 47,
546 e2020GL087360, <https://doi.org/10.1029/2020GL087360>, 2020.
- 547 Puy, A., Borgonovo, E., Lo Piano, S., Levin, S. A., and Saltelli, A.: Irrigated areas drive irrigation water withdrawals, *Nat.*
548 *Commun.*, 12, 4525, <https://doi.org/10.1038/s41467-021-24508-8>, 2021.
- 549 Raes, D., Steduto, P., Hsiao, T., and Fereres, E.: Reference Manual, Chapter3, AquaCrop Model, Version 6.1, FAO, Rome,
550 2018.
- 551 Rodell, M., Velicogna, I., and Famiglietti, J. S.: Satellite-based estimates of groundwater depletion in India, *Nature*, 460, 999-
552 1002, <https://doi.org/10.1038/nature08238>, 2009.
- 553 Rosa, L., Chiarelli, D. D., Rulli, M. C., Dell'Angelo, J., and D'Odorico, P.: Global agricultural economic water scarcity, *Sci.*
554 *Adv.*, 6, eaaz6031, <https://doi.org/10.1126/sciadv.aaz6031>, 2020.
- 555 Siebert, S. and Döll, P.: Quantifying blue and green virtual water contents in global crop production as well as potential
556 production losses without irrigation, *J. Hydrol.*, 384, 198-217, <https://doi.org/10.1016/j.jhydrol.2009.07.031>, 2010.
- 557 SCIO, State Council Information Office: White Paper: the Grain Issue in China, available at:
558 <http://www.scio.gov.cn/zfbps/ndhf/1996/Document/307978/307978.htm>, (last access: 7 March 2023), 1996.
- 559 Steffen, W., Richardson, K., Rockström, J., Cornell, S. E., Fetzer, I., Bennett, E. M., Biggs, R., Carpenter, S. R., De Vries, W.,
560 and De Wit, C. A.: Planetary boundaries: Guiding human development on a changing planet, *Science*, 347, 1259855,
561 <https://doi.org/10.1126/science.1259855>, 2015.
- 562 Tamea, S., Tuninetti, M., Soligno, I., and Laio, F.: Virtual water trade and water footprint of agricultural goods: the 1961–2016
563 CWASI database, *Earth Syst. Sci. Data*, 13, 2025-2051, <https://doi.org/10.5194/essd-13-2025-2021>, 2021.
- 564 Tans, P., and Keeling, R.: Mauna Loa CO2 monthly mean data, <https://gml.noaa.gov/ccgg/trends/data.html>.
- 565 Tilman, D., Balzer, C., Hill, J., and Befort, B. L.: Global food demand and the sustainable intensification of agriculture, *Proc.*
566 *Natl. Acad. Sci. U. S. A.*, 108, 20260-20264, <https://doi.org/10.1073/pnas.1116437108>, 2011.
- 567 Tuninetti, M., Tamea, S., Laio, F., and Ridolfi, L.: A Fast Track approach to deal with the temporal dimension of crop water
568 footprint, *Environ. Res. Lett.*, 12, 074010, <https://doi.org/10.1088/1748-9326/aa6b09>, 2017.
- 569 Tuninetti, M., Tamea, S., D'Odorico, P., Laio, F., and Ridolfi, L.: Global sensitivity of high-resolution estimates of crop water
570 footprint, *Water Resour. Res.*, 51, 8257-8272, <https://doi.org/10.1002/2015WR017148>, 2015.
- 571 Vanuytrecht, E., Raes, D., Steduto, P., Hsiao, T. C., Fereres, E., Heng, L. K., Vila, M. G., and Moreno, P. M.: AquaCrop: FAO's
572 crop water productivity and yield response model, *Environ. Modell. Softw.*, 62, 351-360,
573 <https://doi.org/10.1016/j.envsoft.2014.08.005>, 2014.
- 574 Wada, Y., Wisser, D., Eisner, S., Flörke, M., Gerten, D., Haddeland, I., Hanasaki, N., Masaki, Y., Portmann, F. T., and Stacke,



- 575 T.: Multimodel projections and uncertainties of irrigation water demand under climate change, *Geophys. Res. Lett.*, 40,
576 4626-4632, <https://doi.org/10.1002/grl.50686>, 2013.
- 577 Waha, K., Van Bussel, L., Müller, C., and Bondeau, A.: Climate-driven simulation of global crop sowing dates, *Glob. Ecol.*
578 *Biogeogr.*, 21, 247-259, <https://doi.org/10.1111/j.1466-8238.2011.00678.x>, 2012.
- 579 Water Footprint Network.: WaterStat–water footprint statistics, available at: <https://waterfootprint.org/en/resources/waterstat/>.
580 (last access: 7 March 2023), 2020.
- 581 Wang, W., Zhuo, L., Li, M., Liu, Y., and Wu, P.: The effect of development in water-saving irrigation techniques on spatial-
582 temporal variations in crop water footprint and benchmarking, *J. Hydrol.*, 577, 123916,
583 <https://doi.org/10.1016/j.jhydrol.2019.123916>, 2019.
- 584 Wang, W., Zhuo, L., Ji, X., Yue, Z., Li, Z., Li, M., Zhang, H., Gao, R., Yan, C., Zhang, P., and Wu, P.: CWFETB-China: Gridded
585 dataset of consumptive water footprints, evaporation, transpiration, and associate benchmarks of crop production in China
586 (2000-2018), Zenodo [data set], <https://doi.org/10.5281/zenodo.7756013>, 2023.
- 587 Wang, X., Müller, C., Elliot, J., Mueller, N. D., Ciais, P., Jägermeyr, J., Gerber, J., Dumas, P., Wang, C., and Yang, H.: Global
588 irrigation contribution to wheat and maize yield, *Nat. Commun.*, 12, 1235, <https://doi.org/10.1038/s41467-021-21498-5>,
589 2021.
- 590 Xie, G., Han, D., Wang, X., and Lü, R.: Harvest index and residue factor of cereal crops in China, *Journal of China agricultural*
591 *university*, 16, 1-8, 2011(in Chinese).
- 592 Yin, Y., Tang, Q., Liu, X., and Zhang, X.: Water scarcity under various socio-economic pathways and its potential effects on
593 food production in the Yellow River basin, *Hydrol. Earth Syst. Sci.*, 21, 791-804, [https://doi.org/10.5194/hess-21-791-](https://doi.org/10.5194/hess-21-791-2017)
594 2017, 2017.
- 595 Yue, Z., Ji, X., Zhuo, L., Wang, W., Li, Z., and Wu, P.: Spatiotemporal responses of the crop water footprint and its associated
596 benchmarks under different irrigation regimes to climate change scenarios in China, *Hydrol. Earth Syst. Sci.*, 26, 4637-
597 4656, <https://doi.org/10.5194/hess-26-4637-2022>, 2022.
- 598 Zhang, F. and Zhu, Z.: Harvest index for various crops in China, *Scientia Agricultura Sinica*, 23, 83-87, 1990 (in Chinese).
- 599 Zhuo, L., Mekonnen, M. M., and Hoekstra, A. Y.: The effect of inter-annual variability of consumption, production, trade and
600 climate on crop-related green and blue water footprints and inter-regional virtual water trade: A study for China (1978–
601 2008), *Water Res.*, 94, 73-85, <https://doi.org/10.1016/j.watres.2016.02.037>, 2016a.
- 602 Zhuo, L., Mekonnen, M. M., and Hoekstra, A. Y.: Benchmark levels for the consumptive water footprint of crop production
603 for different environmental conditions: a case study for winter wheat in China, *Hydrol. Earth Syst. Sci.*, 20, 4547-4559,
604 <https://doi.org/10.5194/hess-20-4547-2016>, 2016b.



605 Zhuo, L., Mekonnen, M. M., Hoekstra, A. Y., and Wada, Y.: Inter-and intra-annual variation of water footprint of crops and
606 blue water scarcity in the Yellow River basin (1961–2009), *Adv. Water Resour.*, 87, 29-41,
607 <https://doi.org/10.1016/j.advwatres.2015.11.002>, 2016c.